Research Square

Preprints are preliminary reports that have not undergone peer review.
They should not be considered conclusive, used to inform clinical practice,
or referenced by the media as validated information.

Finger-Specific Electrotactile Sensation and Its Sensorimotor Cortical Substrates During TENS: A Combined Psychophysical and MEG Investigation

Jintao Lai
Shanghai Jiao Tong University
Dekun Yang
Shanghai Jiao Tong University
Yegang Hu
Shanghai Mental Health Center
Jiabei He
West China Hospital of Sichuan University
Jing He
West China Hospital of Sichuan University
Chunlei Shan
Shanghai Jiao Tong University School of Medicine
Ning Jiang
West China Hospital of Sichuan University
Xiaoli Guo
Shanghai Jiao Tong University
Yao Chen
Shanghai Jiao Tong University
Xiaohong Sui
suixhong@sjtu.edu.cn

Shanghai Jiao Tong University

Research Article

Keywords: Keywords: Electrotactile feedback, Finger-specific sensory processing, Somatosensory evoked fields, Sensorimotor connectivity, Cortical source localization, Stroke rehabilitation

Posted Date: August 28th, 2026

DOI: https://doi.org/10.21203/rs.3.rs-10215072/v1

License: This work is licensed under a Creative Commons Attribution 4.0 International License.
Read Full License

Additional Declarations: No competing interests reported.

Finger-Specific Electrotactile Sensation and Its Sensorimotor Cortical Substrates During TENS: A Combined Psychophysical and MEG Investigation

Jintao Lai[1†], MEng, Dekun Yang[1†], MEng, Yegang Hu[2], PhD, Jiabei He[3], MD, Jing He[3], PhD, Chunlei Shan[4, 5] PhD, Ning Jiang[6], PhD, Xiaoli Guo[1], PhD, Yao Chen[1], PhD, Xiaohong Sui[1*], PhD

[1]School of Biomedical Engineering, Shanghai Jiao Tong University, Shanghai, China

[2]Shanghai Mental Health Center, Shanghai Jiao Tong University School of Medicine, Shanghai, China

[3]Department of Rehabilitation Medicine, West China Hospital, Sichuan University, Chengdu, Sichuan, China

[4]Rehabilitation Research Institute, Shanghai Jiao Tong University School of Medicine, Shanghai, China

[5]Department of Rehabilitation Medicine, Tongren Hospital, Shanghai Jiao Tong University School of Medicine, Shanghai, China

[6]National Clinical Research Center for Geriatrics, West China Hospital, Sichuan University, Chengdu, Sichuan, China

Tel: +86-21-34204079; E-mail: suixhong@sjtu.edu.cn

[†] The authors contributed equally to this paper.

* Corresponding author: Xiaohong Sui

Corresponding author's address: Rm. 504, Wenxuan Building, No. 800 Dongchuan Road, Shanghai, China

Corresponding author's phone: +8621-34204079

Corresponding author's e-mail address: suixhong@sjtu.edu.cn

Running head: (limit 50 characters)

finger electrotactile sensation with MEG

Number of words in abstract: (limit 350 words)

Number of words in main text: (limit ~3,000 words)

Number of figures: 11

Number of tables: 0

Acknowledgement statement (including conflict of interest and funding sources):

The authors declare no conflict of interests, and this research is supported by the National Key Research and Development Program of China (Nos. 2022YFC3601103, 2024YFE0200900), the National Natural Science Foundation of China (No. 62176158) and STAR Project of Shanghai Jiao Tong University (20220103).

ABSTRACT

Background: Stroke frequently causes somatosensory impairments that impede upper-limb motor recovery. Although transcutaneous electrical nerve stimulation (TENS) can noninvasively deliver artificial tactile feedback, the normative characteristics of finger-specific electrotactile perception and its underlying sensorimotor cortical mechanisms in healthy individuals remain poorly characterized. This study aimed to establish psychophysical baselines of digit-specific electrotactile sensation and to investigate the corresponding cortical substrates and sensorimotor connectivity patterns using magnetoencephalography (MEG).

Methods: Sixteen right-handed healthy adults (10 males, 6 females; aged 22–30 years) completed psychophysical assessments. Perception thresholds and just-noticeable differences (JNDs) for electrotactile stimulation were quantified across all ten digits using a two-alternative forced-choice paradigm. Eight participants subsequently underwent whole-head MEG recordings during TENS applied to the bilateral thumbs and ring fingers—digits exhibiting distinct psychophysical thresholds. Somatosensory evoked fields (SEFs) were analyzed for early-response peak latency and amplitude, cortical sources were localized using equivalent current dipole modeling, and sensorimotor functional connectivity was assessed via imaginary coherence analysis in the alpha (8–13 Hz) and beta (13–40 Hz) bands. Data were analyzed using repeated-measures ANOVA with Bonferroni-corrected post hoc comparisons.

Results: Electrotactile perception thresholds differed significantly across digits ($F = 7.08$, $p < 0.001$, partial $\eta^2 = 0.392$), with the right thumb exhibiting markedly higher thresholds than both left and right ring fingers (Bonferroni-corrected $p < 0.001$). A significant hand × digit interaction was observed ($F = 3.10$, $p = 0.025$). In contrast, Weber fractions did not vary significantly across hands or digits. MEG recordings consistently revealed early cortical responses (tens of ms post-stimulus) across all stimulation sites, with responses localized contralaterally to the stimulated digits. Group-level early-response peak latency and amplitude did not differ significantly across stimulation sites; however, the right ring finger showed a site-specific negative correlation between the latency and amplitude ($r = -0.85$, $p = 0.016$). TENS transiently enhanced sensorimotor imaginary coherence across all stimulated digits, with peak modulation occurring 100–200 ms post-stimulation. Connectivity increases were consistently higher in the alpha band than in the beta band and followed a stable pathway hierarchy: contralateral–ipsilateral somatosensory > somatosensory–motor cortex coupling.

Conclusions: Finger-specific electrotactile detection sensitivity varies across digits in healthy adults, with the frequently used right thumb showing higher detection thresholds. TENS engages not only early somatosensory cortical responses but also transient alpha- and beta-band sensorimotor network coupling. These findings provide a normative psychophysical and neurophysiological framework for developing individualized, digit-specific TENS protocols, with potential applications in post-stroke sensorimotor rehabilitation.

Trial registration: Not applicable (healthy participant study without interventions for disease treatment).

KEYWORDS

Keywords: Electrotactile feedback; Finger-specific sensory processing; Somatosensory evoked fields; Sensorimotor connectivity; Cortical source localization; Stroke rehabilitation

INTRODUCTION

Stroke ranks as the third-leading cause of death and disability worldwide, accounting for a substantial burden of disease as measured by disability-adjusted life-years (DALYs). The global economic impact of stroke exceeds US$721 billion, representing 0.66% of the world's GDP, with an estimated 100 million people affected globally[1]. In China, the stroke burden is substantial, with approximately 28.76 million current patients, 4 million new cases annually, and 2.19 million stroke-related deaths each year [2]. This devastating condition represents the third most common cause of mortality in China, and is responsible for 45.9 million DALYs[2]. Similarly, the United States faces a significant stroke burden, with about 795,000 new cases reported annually[3].

In China, approximately 70% of stroke survivors require physical rehabilitation to address movement disorders such as dyskinesia, making motor function restoration a key focus in clinical rehabilitation. Concurrently, 50% - 80% of patients suffer from somatosensory impairments[4]. Clinically, the loss or impairment of upper-limb somatosensation —including proprioception and touch—can significantly hinder fine motor control, object manipulation, or hand movement dexterity in stroke survivors, ultimately compromising motor functional recovery[5-8]. Anatomically, the somatosensory and motor cortices are separated by the central sulcus, which allows the somatosensory signals to reach out to the proximal motor counterpart rapidly, facilitating more efficient and intuitive limb movement control. A review of fourteen randomized clinical trials on BCI-based motor rehabilitation revealed that somatosensory impairments generally hinder motor rehabilitation outcomes by impairing motor learning, skill acquisition, and functional use of the affected limb [9].

Supporting this, Rong Li et al. demonstrated that somatosensory evoked potentials (SEPs) were closely correlated with fine motor function recovery, as measured by Montoya staircase test in a rat model of cervical spinal cord injury [10]. Notably, finger sensation plays a pivotal role in fine motor control [11]. Fine motor skills such as object grasping, pinching, and precise manipulation all rely on accurate finger tactile perception. Therefore, restoring or enhancing finger tactile perception post stroke is crucial to effective fine motor control rehabilitation.

Noninvasive artificial tactile sensation can be delivered via vibration or transcutaneous electrical nerve stimulation (TENS) [12-16]. Compared with tactile vibration, TENS offers several distinct advantages, including richer perception modalities, effortless recognition, greater design flexibility, and finer spatial resolution. These characteristics make TENS more suitable for precise assessment of finger tactile perception and subsequent application in stroke rehabilitation. It is worth noting that stroke can cause heterogeneous somatosensory deficits across distinct hand regions tested with calibrated monofilaments[17]. Consequently, assessing finger-specific electrotactile sensation in healthy individuals is essential to establish normative physiological baselines for fingertip sensory processing, including differentiated perceptual thresholds and modulatory effects on sensorimotor cortical connectivity.

Magnetoencephalography (MEG), with its high temporal and spatial resolution, is well suited for investigating brain responses to sensory stimulation [18-20]. Previous studies have employed MEG to examine the phantom-limb sensations induced by TENS in amputees[21], and to study the somatosensory evoked fields in the hemiplegic side of stroke patients under pneumatic stimulation and passive movement [22] . However, to the best of our knowledge, no studies to date have used MEG to characterize cortical responses across different fingers with distinct sensory perception thresholds. This research gap indicates that the current understanding of sensorimotor connectivity of finger-specific electrotactile perception is still insufficient. Therefore, conducting psychophysical experiments to evaluate the perceptual thresholds of TENS on fingers in healthy individuals, combined with MEG to explore the corresponding cortical responses, is not only an important step to fill this research gap but also will be an inevitable requirement to improve the theoretical system of stroke somatosensory rehabilitation and promote the development of clinical rehabilitation technology.

To this end, the present study employed psychophysical experiments in healthy participants to investigate electrotactile discrimination across the ten fingers during TENS, by quantifying perception thresholds and intensity-based just-noticeable differences. Furthermore, MEG was adopted to explore the neural mechanisms underlying artificial finger

sensation and its influence on sensorimotor coupling, through analysis of somatosensory evoked fields (SEFs) elicited by TENS applied to fingers exhibiting markedly distinct perception thresholds.

METHODS

SUBJECTS

Sixteen right-handed healthy adults (10 males and 6 females; age range, 22–30 years) were enrolled in the psychophysical experiment. Of these participants, 8 individuals (6 males and 2 females) further completed magnetoencephalography (MEG) recordings. All participants reported no history of neurological or psychiatric disorders. Participants were recruited from volunteers responding to advertisements distributed through social media and university bulletin boards.

All participants provided written informed consent before the experiment. The consent form described the study purpose, experimental procedures, and potential risks. Participants were informed that they could withdraw from the study at any time without penalty. The study was conducted in accordance with the Declaration of Helsinki and was approved by the institutional review boards of Shanghai Jiao Tong University (No. B20230256) and West China Hospital, Sichuan University (No. 2024 Review (607) & (644)). Participant confidentiality was protected by pseudonymized coding and secure data storage.

PSYCHOPHYSICAL ASSESSMENT OF ELECTROTACTILE SENSATION

STIMULATION SETUP

A four-channel electrostimulator (STG 4004, Multichannel Systems, Reutlingen, Germany) was used to deliver constant-current transcutaneous electrical stimulation. Pulse amplitude was adjusted in 2 μA steps. Stimulation was delivered through custom-made MEG-compatible flexible carbon-fiber non-woven electrodes with hydrogel-coated contact surfaces (diameter, 5 mm). For each digit, the active electrode was placed on the fingertip, and the return electrode was positioned on the distal phalanx. Transcutaneous electrical stimulation has been widely used for artificial tactile feedback and non-invasive sensory substitution because it can activate cutaneous afferent pathways without implanted interfaces [12–16,21,23,24].

PERCEPTION THRESHOLD MEASUREMENT

All 16 participants completed a tactile perception (also referred to as detection) threshold assessment for all ten digits employing a two-alternative forced-choice paradigm[23, 24] widely adopted in psychophysical experiments. As illustrated in Figure 1a, participants maintained a comfortable posture while viewing a computer screen and making perceptual judgments. The paradigm consisted of two observation intervals per trial (Figure 1c) to discriminate detection thresholds; each interval presented either a null stimulus or an active stimulation (Figure 1b). In each 5-second trial, two windows displayed cross cues: the left window showed a fixed cross throughout 0-2 s with an attention prompt (0-1 s) followed by a stimulus (1-2 s), while the right window displayed a fixed cross throughout 3-5 s with an attention prompt (3-4 s) and stimulus delivery (4-5 s). This carefully synchronized design ensured precise temporal alignment between visual cues and tactile stimulation events (Figure 1c).

Participants were instructed to identify the target stimulus across two distinct temporal windows. As illustrated in Figure 1b, the stimuli featured adjustable pulse amplitudes calibrated individually to each participant's perceptual threshold range, while maintaining a constant frequency of 50 Hz and pulse width of 200 μs to generate near-natural tactile perceptions. Detection thresholds were subsequently determined by fitting psychometric functions to experimental response data (Figure 1d), operationally defined as the stimulus amplitude yielding a 75% correct response rate. This experimental paradigm enables quantitative evaluation of electrotactile discrimination performance, facilitates robust and reliable quantification of tactile detection thresholds, and allows for precise modulation of stimulus presentation parameters and temporal delivery.

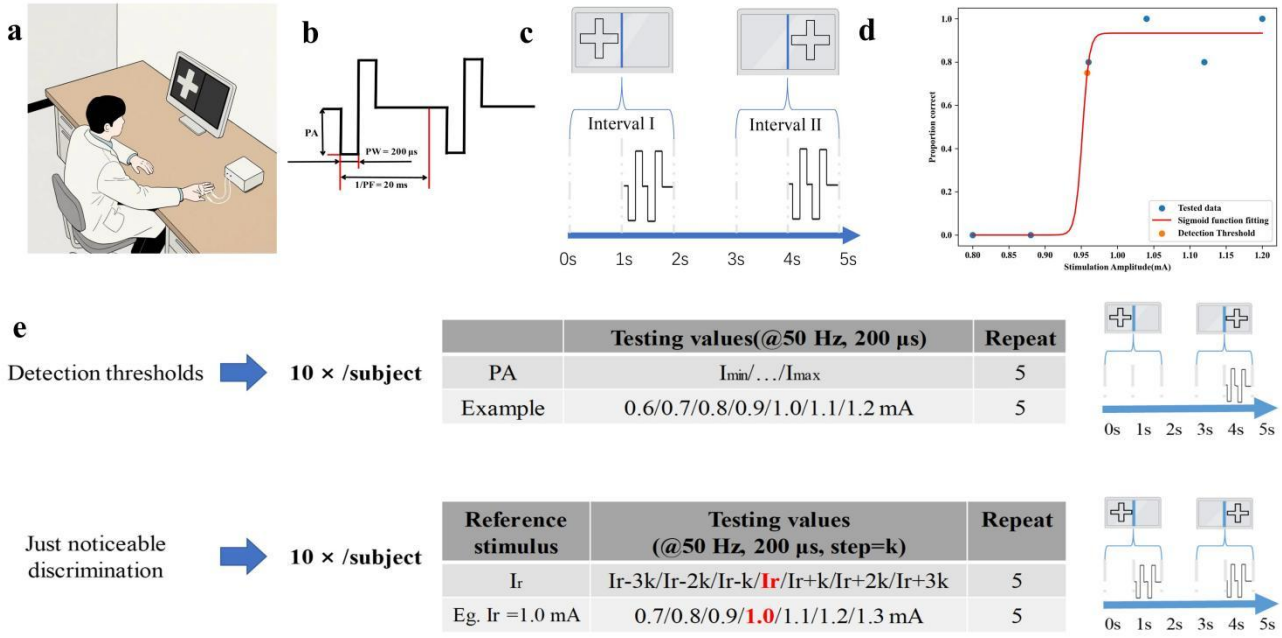


Fig.1 Schematic of the psychophysical experiment under TENS. **a.** Experimental setup; **b.** Diagram of electrical stimulus parameters, where pulse amplitude represents stimulation intensity, with a constant pulse frequency of 50 Hz and pulse width of 200 μs; **c.** Two successive observation intervals per trial, containing one inactive null stimulus and one active electrical stimulus; **d.** Tactile detection threshold estimated via psychometric function fitting, defined at 75% correct discrimination accuracy; **e.** Protocols of two experiments: detection threshold measurement (**top**) and just noticeable difference discrimination (**bottom**). Pulse amplitude (PA) was modulated at fixed PF = 50 Hz and PW = 200 μs. Stimulation trials were pseudo-randomized within each block, with an inter-trial interval of approximately 2 s.

JUST NOTICEABLE DIFFERENCE

Although electrical stimulation parameters can be precisely modulated, human perceptual systems do not necessarily exhibit correspondingly high-resolution discrimination performance. Accordingly, it is critical to quantify human perceptual sensitivity to variations in stimulus intensity. In psychophysical research, the Just-Noticeable Difference (JND) is widely adopted as a core metric, referring to the minimal detectable change in stimulus parameters that produces a perceptible difference relative to a given reference stimulus. A two-alternative forced-choice (2AFC) paradigm was implemented to assess JND values for electrotactile discrimination.

Throughout the experiment, participants were instructed to identify the stronger stimulus between the test and reference stimuli in each trial, following the experimental paradigm reported by Li et al. [23]. Participant responses were subsequently converted into corresponding probe metrics according to their discrimination accuracy for the more intense stimulus. A sigmoid function was fitted to the collected response data, with the upper and lower asymptotes constrained to 75% and 25% correct response probability, respectively. For each given reference stimulus, the JND was derived as follows:

$$\frac{(I - I_l) + (I_u - I)}{2} = JND \tag{1}$$

where I denotes the reference stimulus intensity, and I_u and I_l represent the upper and lower discrimination thresholds, respectively.

Weber's law states that the ratio of the minimal detectable stimulus change to the baseline stimulus intensity remains constant for a given sensory modality. This ratio, defined as the Weber fraction (k)[25], is formulated in Equation (2). This fundamental principle underpins the theoretical quantification of the relationship between stimulus intensity and perceptual discrimination sensitivity.

$$\frac{(I - I_l) + (I_u - I)}{2 \times I} = k \tag{2}$$

MEG Experiment

MEG Recording Setup

Whole-brain MEG data were acquired using a helmet-shaped whole-head MEG system (Elekta Neuromag TRIUX, Finland) in a magnetically shielded room. The system consisted of 306 channels distributed across 102 sensor locations, with one magnetometer and two orthogonally oriented planar gradiometers at each location. Continuous MEG signals were sampled at 1000 Hz. MEG is well suited for investigating somatosensory processing because it provides millisecond-level temporal resolution and enables non-invasive characterization of cortical responses to sensory stimulation [18–20,22].

Before recording, four head-position indicator coils were attached to predefined cranial landmarks, with two coils placed on the forehead and two posterior to the ears. A Polhemus 3D digitization system (Colchester, NH, USA) was used to

digitize the locations of the coils, three anatomical fiducial points (nasion and bilateral preauricular points), and approximately 100 additional scalp points. Participants were then seated in the shielded room and instructed to minimize head movement throughout recording.

High-resolution T1-weighted structural MRI data were acquired using a 3T Siemens MAGNETOM Verio scanner (Erlangen, Germany) with a 32-channel head coil. Structural images were acquired at an isotropic resolution of 1 × 1 × 1 mm^3 and used for MEG–MRI co-registration and source localization.

MEG Stimulation Paradigm

Based on the psychophysical results, the thumbs and ring fingers of both hands were selected for MEG stimulation because these digits showed distinct electrotactile threshold profiles. Charge-balanced biphasic square-wave current pulses were delivered using a DS7A stimulator (Digitimer, UK). Pulse duration was fixed at 200 μs, consistent with the psychophysical experiment.

The stimulation frequency was set to 2 Hz to allow cortical evoked responses to return toward baseline between successive stimuli. For each participant and each stimulation site, the stimulation current used during MEG acquisition was set to twice the individually measured perception threshold, while remaining within the participant's comfort range. MEG recordings were completed in 8 participants.

MEG Data Processing

MEG data were processed through three main steps: MEG–MRI co-registration, source reconstruction and localization, and extraction of cortical time series from sensorimotor regions. Analyses were conducted using Brainstorm within the MATLAB environment, together with FieldTrip and custom analysis scripts. Cortical regions of interest were defined according to the Desikan–Killiany parcellation, with emphasis on the precentral and postcentral cortices. Fig 2 illustrates a comprehensive flowchart of the entire MEG data processing pipeline.

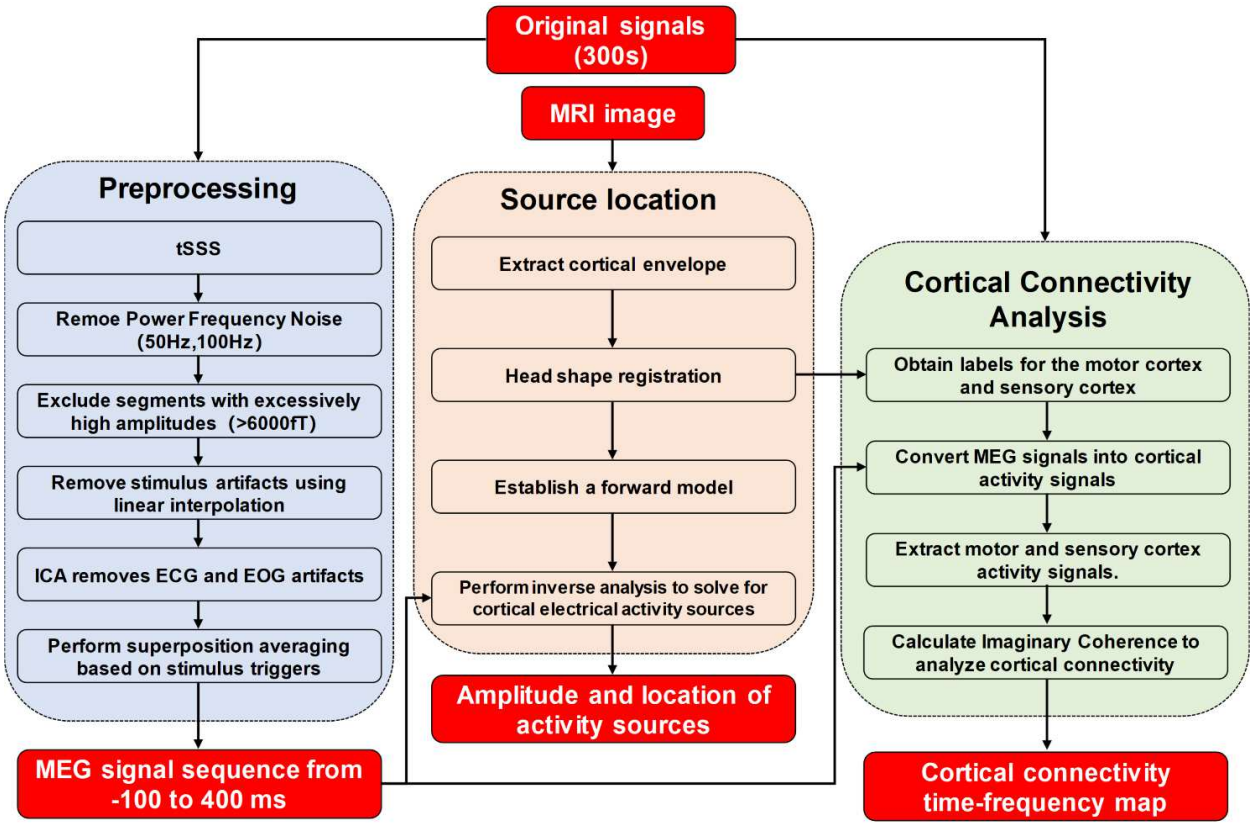


Fig. 2. MEG data processing pipeline

PREPROCESSING

Raw MEG data were acquired with an online passband of 0.01–330 Hz and a sampling rate of 1000 Hz. Continuous data were bandpass-filtered from 0.5 to 60 Hz. Notch filters at 50 and 100 Hz were applied to reduce power-line interference. Independent component analysis was then used to attenuate ocular and cardiac artifacts associated with electro-oculographic and electrocardiographic activity. Data segments with amplitudes exceeding 6000 fT were rejected to reduce contamination from gross movement or non-physiological artifacts.

For stimulus-locked analyses, epochs were extracted from −0.1 to 0.4 s relative to stimulus onset. These epochs were used to characterize somatosensory evoked fields, early-response peak latency and amplitude, source localization, and post-stimulation functional connectivity.

SOURCE LOCATION

Source localization was performed using an overlapping-sphere forward model and an equivalent current dipole (ECD) inverse approach. Fixed-dipole modelling was used to compare cortical response locations across stimulation sites. Moving-dipole modelling was used to characterize the temporal trajectory of cortical source activity within a given stimulation condition. Only dipoles with a goodness-of-fit value greater than 70% were retained for subsequent interpretation.

Individual structural MRI data were processed and integrated into the source estimation workflow. Source localization was conducted with Brainstorm and FieldTrip to support MEG–MRI co-registration, dipole fitting, and visualization of cortical response patterns.

FUNCTIONAL CONNECTIVITY ANALYSIS

To assess TENS-induced modulation of sensorimotor cortical coupling, imaginary coherence was calculated between cortical time series extracted from somatosensory and motor regions. Imaginary coherence was selected because it is less sensitive to volume conduction and zero-lag spurious correlations than conventional coherence [26–28].

Connectivity analyses focused on the 8–40 Hz range and were further examined in the alpha (8–13 Hz) and beta (13–40 Hz) bands, given the known involvement of sensorimotor alpha- and beta-band oscillations in tactile attention and sensorimotor processing [29]. The contralateral somatosensory cortex (SC-C) was used as the reference region, and its connectivity with the ipsilateral somatosensory cortex (SC-I), contralateral motor cortex (MC-C), and ipsilateral motor cortex (MC-I) was quantified. Connectivity was compared between the pre-stimulation baseline window (−100 to 0 ms) and four post-stimulation windows (0–100, 100–200, 200–300, and 300–400 ms).

STATISTICAL ANALYSIS

Psychophysical data were analysed using repeated-measures ANOVA. Electrotactile perception thresholds were analysed using a 2 (hand: left, right) × 5 (digit: five digits) repeated-measures design. Weber fractions were analysed using the same 2 × 5 design. When significant effects were detected, Bonferroni-corrected post hoc comparisons were performed.

MEG early-response peak latency and amplitude were analysed using a 2 (hand: left, right) × 2 (digit: thumb, ring finger) repeated-measures ANOVA. Correlations among perception threshold, early-response peak latency, and early-response peak amplitude were evaluated using Pearson and Spearman correlation analyses in participants with complete

psychophysical and MEG datasets. Functional connectivity changes were evaluated by comparing post-stimulation imaginary coherence values with pre-stimulation baseline values across frequency bands, time windows, stimulation sites, and connectivity pathways.

RESULTS

PERCEPTION THRESHOLD AND JUST NOTICEABLE DIFFERENCE

A total of 16 participants completed the psychophysical experiment. Because some participants did not complete measurements for all digits (e.g., due to fatigue during testing or failure of quality control for individual digits), complete electrotactile threshold data from 12 participants and complete Weber fraction data from 9 participants were included in the repeated-measures ANOVA.

For electrotactile perception thresholds, a 2 (hand: left vs. right) × 5 (digit: five digits) repeated-measures ANOVA was conducted in 12 participants. The main effect of hand approached statistical significance ($F = 4.38$, $p = 0.060$, partial $\eta^2 = 0.285$), with lower thresholds in the left hand than in the right hand. The main effect of digit was significant ($F = 7.08$, $p < 0.001$, partial $\eta^2 = 0.392$). Post hoc comparisons showed that the ring finger had significantly lower electrotactile thresholds than the thumb (Bonferroni-corrected $p < 0.001$). A significant hand × digit interaction was also observed ($F = 3.10$, $p = 0.025$, partial $\eta^2 = 0.220$). Post hoc analyses further indicated that the electrotactile thresholds of the left little finger (Bonferroni-corrected $p = 0.007$), left ring finger (Bonferroni-corrected $p = 0.005$), and right ring finger (Bonferroni-corrected $p = 0.005$) were significantly lower than that of the right thumb. The repeated-measures ANOVA results for electrotactile thresholds are shown in Fig. 3.

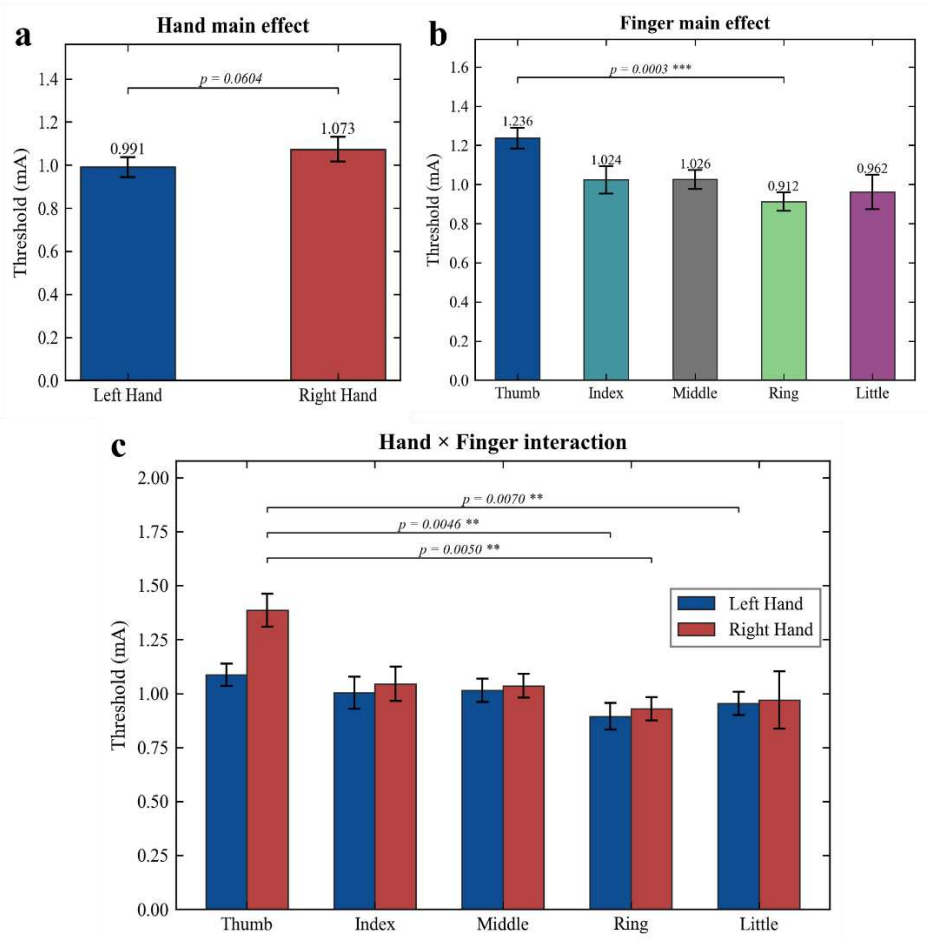


Fig. 3. Repeated-measures ANOVA results for electrotactile perception thresholds. (a) Main effect of hand; (b) main effect of digit; (c) hand × digit interaction.

For Weber fractions, a 2 (hand: left vs. right) × 5 (digit: five digits) repeated-measures ANOVA was conducted in 9 participants. No significant main effect of hand was observed ($F = 1.096$, $p = 0.326$, partial $\eta^2 = 0.121$). The main effect of digit was also not significant ($F = 1.301$, $p = 0.291$, partial $\eta^2 = 0.140$), and no significant hand × digit interaction was detected ($F = 0.651$, $p = 0.630$, partial $\eta^2 = 0.075$). The repeated-measures ANOVA results for Weber fractions are shown in Fig. 4.

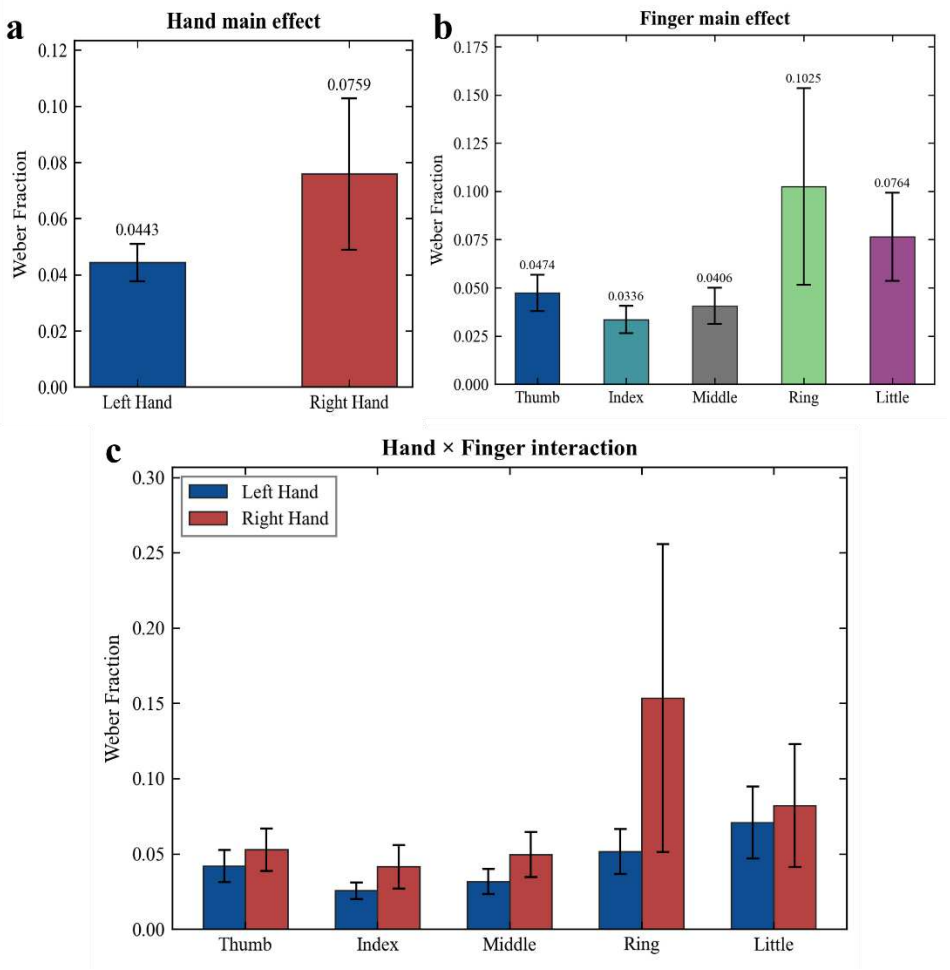


Fig. 4. Repeated-measures ANOVA results for Weber fractions. (a) Main effect of hand; (b) main effect of digit; (c) hand × digit interaction.

TEMPORAL AND SPATIAL CHARACTERIZATION OF MEG SIGNALS

On the basis of the psychophysical results obtained from healthy participants, the left and right thumbs and ring fingers were selected for the MEG experiment to investigate cortical neural responses evoked by transcutaneous electrical stimulation of the digits. In total, 8 healthy participants completed MEG recordings during finger stimulation.

Analysis of somatosensory evoked fields (SEFs) showed that transcutaneous electrical stimulation reliably elicited a prominent response at approximately 35-70 ms after stimulation, corresponding to the early-response peak. As a representative example, Fig. 5a shows the SEF response evoked by transcutaneous electrical nerve stimulation (TENS) of the left thumb in Participant 1. Consistent with the left-hand stimulation paradigm, the MEG sensor topography showed a

clear signal peak over the right cerebral hemisphere, corresponding to the contralateral primary somatosensory cortex (Fig. 5b). The waveform was recorded from 100 ms before to 300 ms after stimulus onset, thereby capturing the temporal evolution of the MEG response.

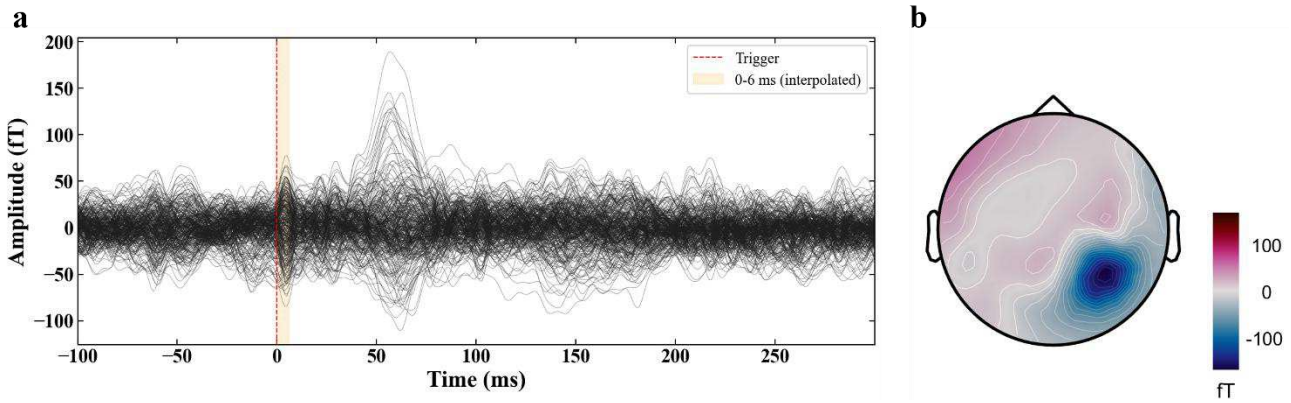


Fig. 5. Somatosensory evoked fields induced by left-hand electrical stimulation in Participant 1. (a) Temporal dynamics of SEFs across the 306-channel sensor array; (b) spatial topography of the peak SEF response in representative channels.

Early-response peak latency (ms) and peak amplitude (fT) were measured in the 8 participants who underwent MEG recordings. A 2 (hand: left vs. right) × 2 (digit: ring finger vs. thumb) repeated-measures ANOVA was then performed. For early-response peak latency, neither the main effect of hand ($F = 0.272$, $p = 0.618$, partial $\eta^2 = 0.037$) nor the main effect of digit ($F = 0.227$, $p = 0.648$, partial $\eta^2 = 0.031$) reached statistical significance. The hand × digit interaction was also not significant ($F = 4.143$, $p = 0.081$, partial $\eta^2 = 0.372$; Fig. 6a). For early-response peak amplitude, no significant main effect of hand ($F = 2.29$, $p = 0.174$, partial $\eta^2 = 0.247$), main effect of digit ($F = 1.97$, $p = 0.203$, partial $\eta^2 = 0.220$), or hand × digit interaction ($F = 2.99$, $p = 0.128$, partial $\eta^2 = 0.299$) was observed (Fig. 6b).

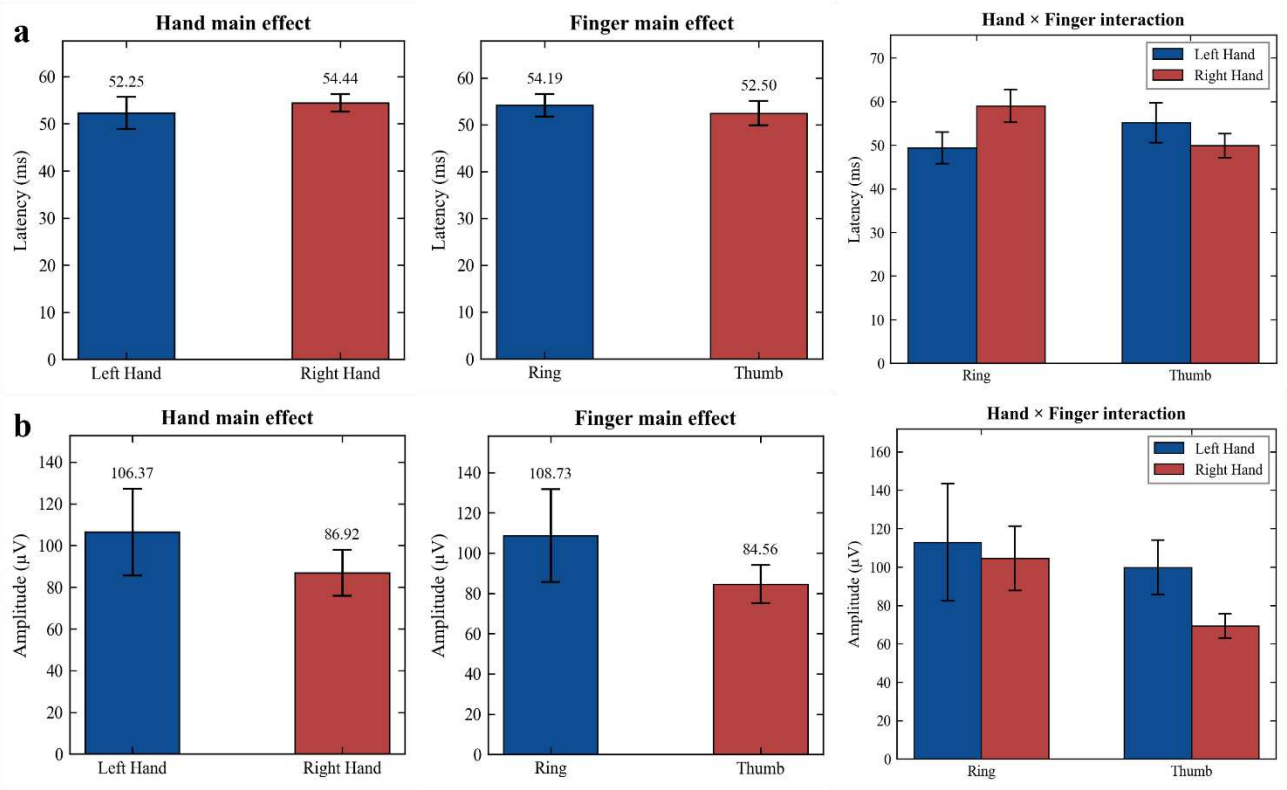


Fig. 6. Repeated-measures ANOVA results for early-response peak. (a) early-response peak latency; (b) early-response peak amplitude.

Correlation analyses were further conducted in 7 participants who had complete psychophysical data and MEG recordings. At the overall level, latency, amplitude, and perception threshold were mutually independent across 28 observations, with no significant linear or monotonic correlations. Specifically, the correlation between latency and amplitude was not significant (Pearson $r = 0.187$, $p = 0.340$; Spearman $\rho = 0.130$, $p = 0.510$). The correlation between latency and threshold was also not significant (Pearson $r = -0.231$, $p = 0.238$; Spearman $\rho = -0.231$, $p = 0.238$). Similarly, no significant correlation was found between amplitude and threshold (Pearson $r = -0.131$, $p = 0.505$; Spearman $\rho = -0.140$, $p = 0.477$). Scatter plots with regression lines for latency, amplitude, and threshold are presented in Fig. 7.

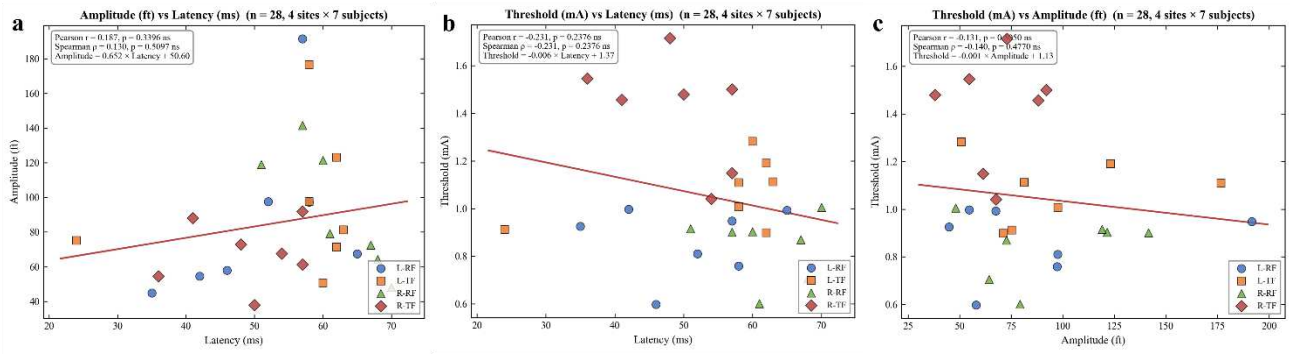


Fig. 7. Scatter plots and regression analyses. (a) Latency versus amplitude; (b) latency versus threshold; (c) amplitude versus threshold.

The correlation matrix among latency, amplitude, and threshold is shown in Fig. 8. Notably, the right ring finger exhibited a site-specific pattern that differed from the other stimulation sites. For this digit, latency was strongly and negatively correlated with amplitude ($r = -0.85$, $p = 0.016$), indicating that shorter neural response latency was associated with larger evoked response amplitude. This relationship was not observed at the other three stimulation sites, suggesting a stimulation-site-specific coupling between response timing and response magnitude.

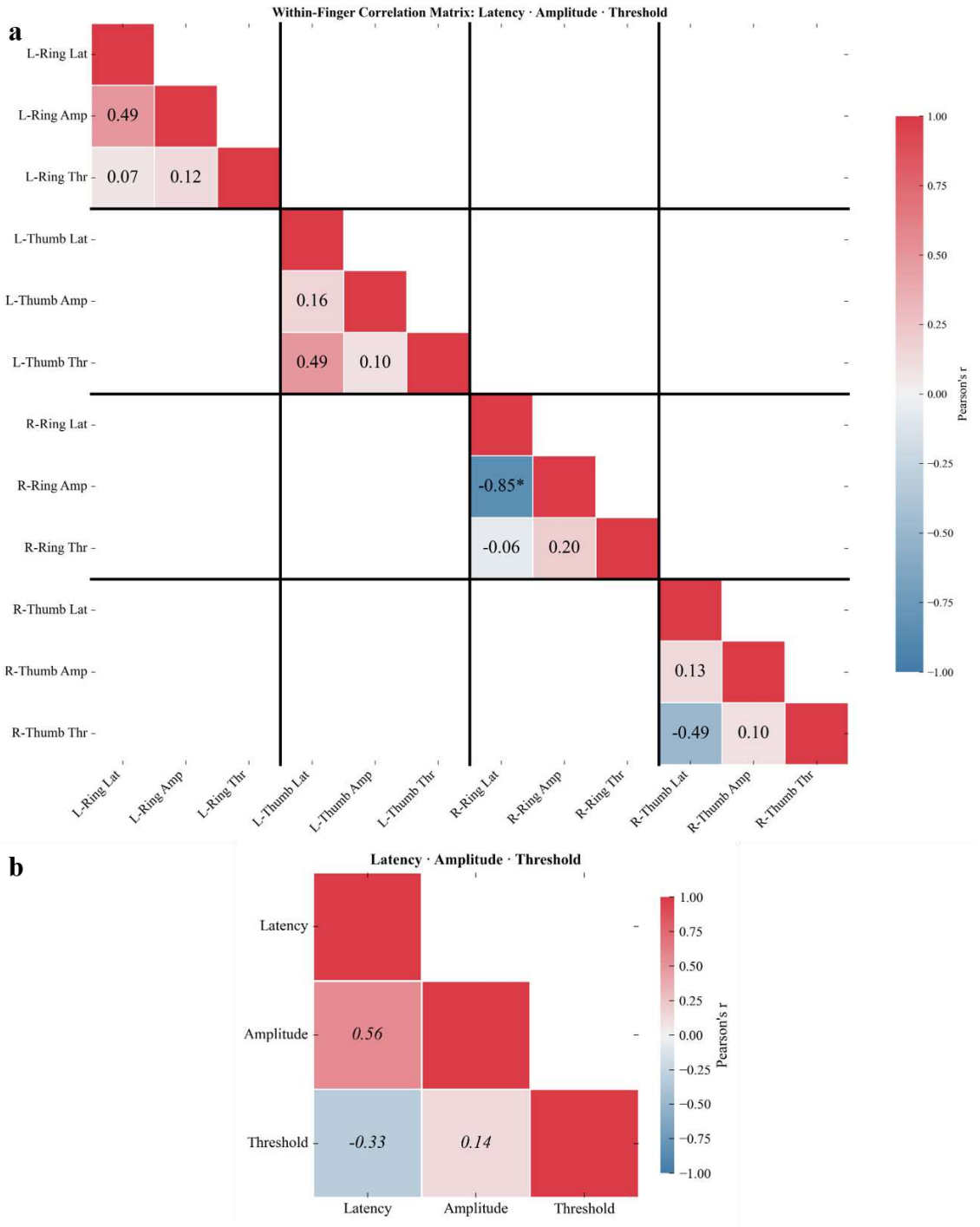


Fig. 8. Correlation matrices for latency, amplitude, and electrotactile threshold. (a) Pearson correlation matrix of 12 variables (4 stimulation sites × 3 measures), with correlation coefficients and significance levels shown in the lower triangle (*p < 0.05, **p < 0.01, ***p < 0.001); black lines separate latency, amplitude, and threshold modules. (b) Aggregated correlation matrix among the three measures.

Source localization was then performed using MEG data from the 8 participants. A fixed-dipole model revealed distinct cortical activation patterns across stimulation sites. Figure 9a showed the cortical response locations induced by transcutaneous electrical nerve stimulation of four digits in one representative participant. Across stimulation sites, responses were localized to brain regions contralateral to the stimulated digits. Across the 8 participants, compared with the ring finger, the thumb, which showed higher perception thresholds, showed response locations closer to the superficial region of the tactile cortex.

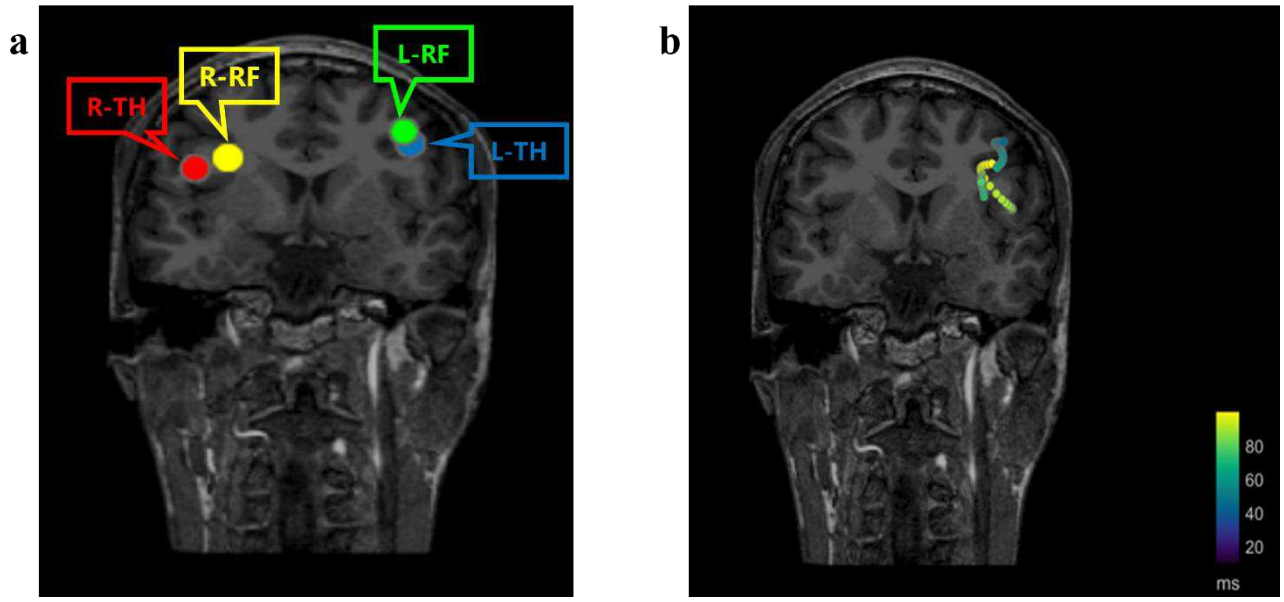


Fig. 9. Cortical source locations reconstructed using fixed- and moving-dipole models during digit transcutaneous electrical stimulation. (a) Fixed dipole source results for Participant 1; (b) Temporal dynamics of moving dipole sources in Participant 1 elicited by left ring finger stimulation.

A moving-dipole model was further used to characterize temporal changes in cortical source locations within the same stimulation site, thereby tracking the trajectory of neural source activity after transcutaneous electrical stimulation. Fig. 9b shows the inverse solution results from 10 to 100 ms after trigger onset for left-ring-finger stimulation in Participant 1. Each small circle represents the dipole location estimated at a specific millisecond. All moving dipoles had goodness-of-fit values above 70%, supporting the reliability of the source estimates. The moving-dipole results traced the temporal evolution of dipole locations after stimulation. Most dipoles were clustered around the central sulcus and postcentral gyrus, corresponding to the primary somatosensory cortex (SI). At approximately 40 - 60 ms, the dipole locations showed a marked shift toward deeper brain regions, away from SI.

CORTICAL CONNECTIVITY UNDER TENS

To characterize TENS-mediated changes in interregional functional connectivity, oscillatory imaginary coherence in the 8–40 Hz range was analyzed between sensorimotor cortical regions. Cortical connectivity was compared between pre- and post-stimulation conditions to identify the main features of TENS-induced neural coupling. Figures 10 and 11 show the dynamic changes in imaginary coherence between the contralateral somatosensory cortex (SC-C) and three other cortical regions in the alpha band (8–13 Hz) and beta band (13–40 Hz), respectively. The three connectivity pathways were: (a) contralateral somatosensory cortex to ipsilateral somatosensory cortex (SC-C ↔ SC-I); (b) contralateral somatosensory cortex to contralateral motor cortex (SC-C ↔ MC-C); and (c) contralateral somatosensory cortex to ipsilateral motor cortex (SC-C ↔ MC-I). For each subplot, data were grouped by stimulation site (left ring finger, left thumb, right ring finger, and right thumb). Each group included five bars representing baseline (−100–0 ms, pre-TENS, normalized to 100%) and four post-TENS time windows (0–100 ms, 100–200 ms, 200–300 ms, and 300–400 ms). Percentages above the bars indicate changes relative to baseline, and asterisks denote statistical significance compared with baseline (*$p < 0.05$, **$p < 0.01$, ***$p < 0.001$).

Across all stimulated digits, cortical connectivity increased markedly after stimulation, with the strongest average connectivity observed during the 100–200 ms post-stimulation window. The right ring finger showed the slowest recovery pattern. Unlike the other digits, its average connectivity remained significantly different from baseline during the 300–400 ms window, particularly for SC-C ↔ SC-I and SC-C ↔ MC-C connectivity. This prolonged connectivity modulation was consistent with the longer latency observed for the right ring finger in the early-response peak analysis.

Frequency-dependent differences were also evident. Absolute imaginary coherence values were consistently higher in the alpha band than in the beta band across all connectivity pathways, digits, and time windows. Post-TENS modulation of sensorimotor connectivity persisted across the entire 0–400 ms post-stimulation period. Statistical significance, predominantly at $p < 0.001$ with a few comparisons at $p < 0.01$, confirmed robust connectivity differences among the three pathways. No significant lateralization effect was observed, as connectivity strength and significance were comparable between homologous pathways for left- and right-digit stimulation. In addition, the relative connectivity strength remained

stable across all five time windows, following the pattern SC-C ↔ SC-I > SC-C ↔ MC-C > SC-C ↔ MC-I. This stable hierarchy indicates consistent temporal modulation of sensorimotor networks following TENS.

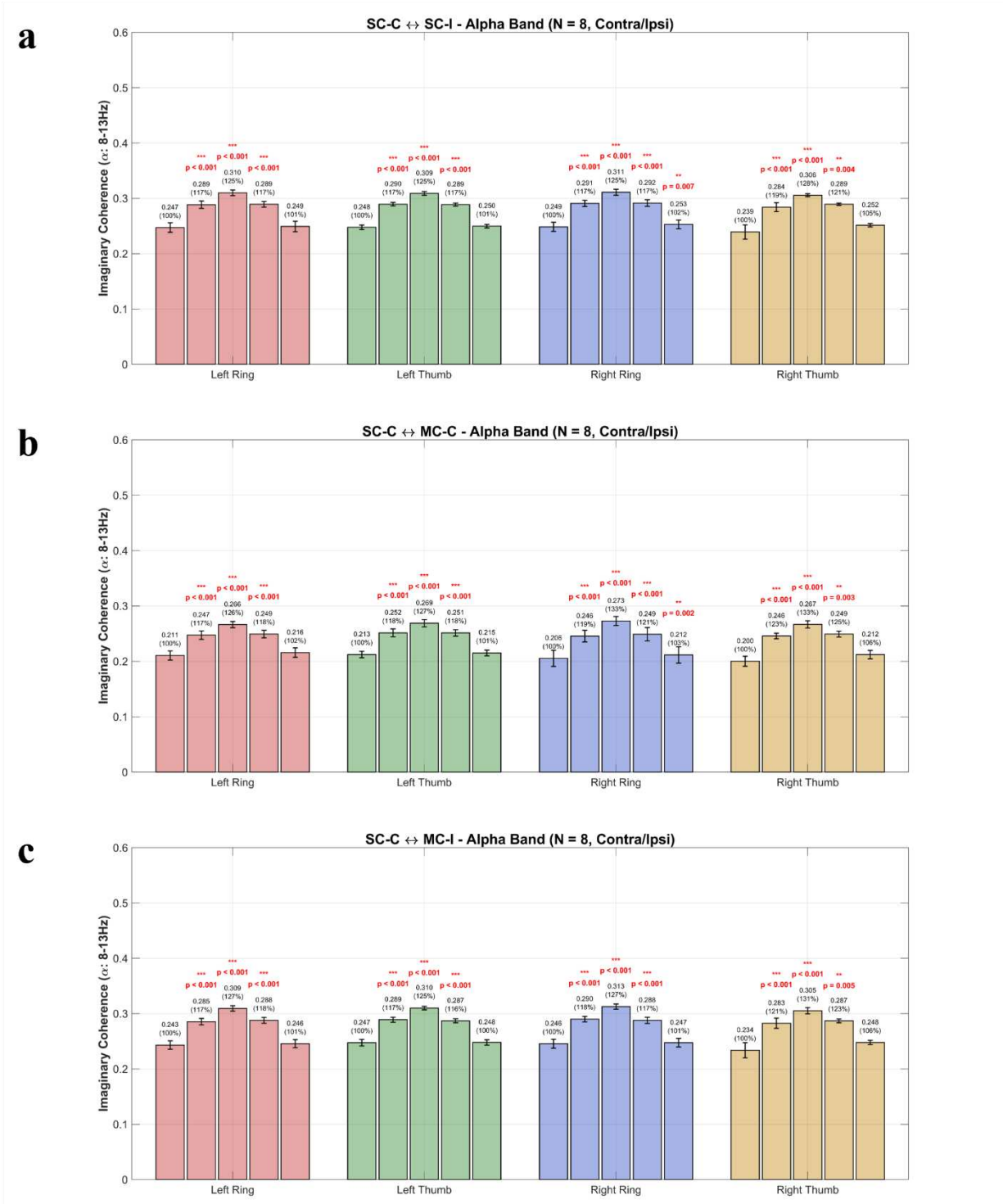


Fig. 10. Changes in imaginary coherence between the contralateral somatosensory cortex (SC-C) and three cortical regions in the alpha band (8–13 Hz) before and after TENS. (a) SC-C ↔ SC-I; (b) SC-C ↔ MC-C; (c) SC-C ↔ MC-I.

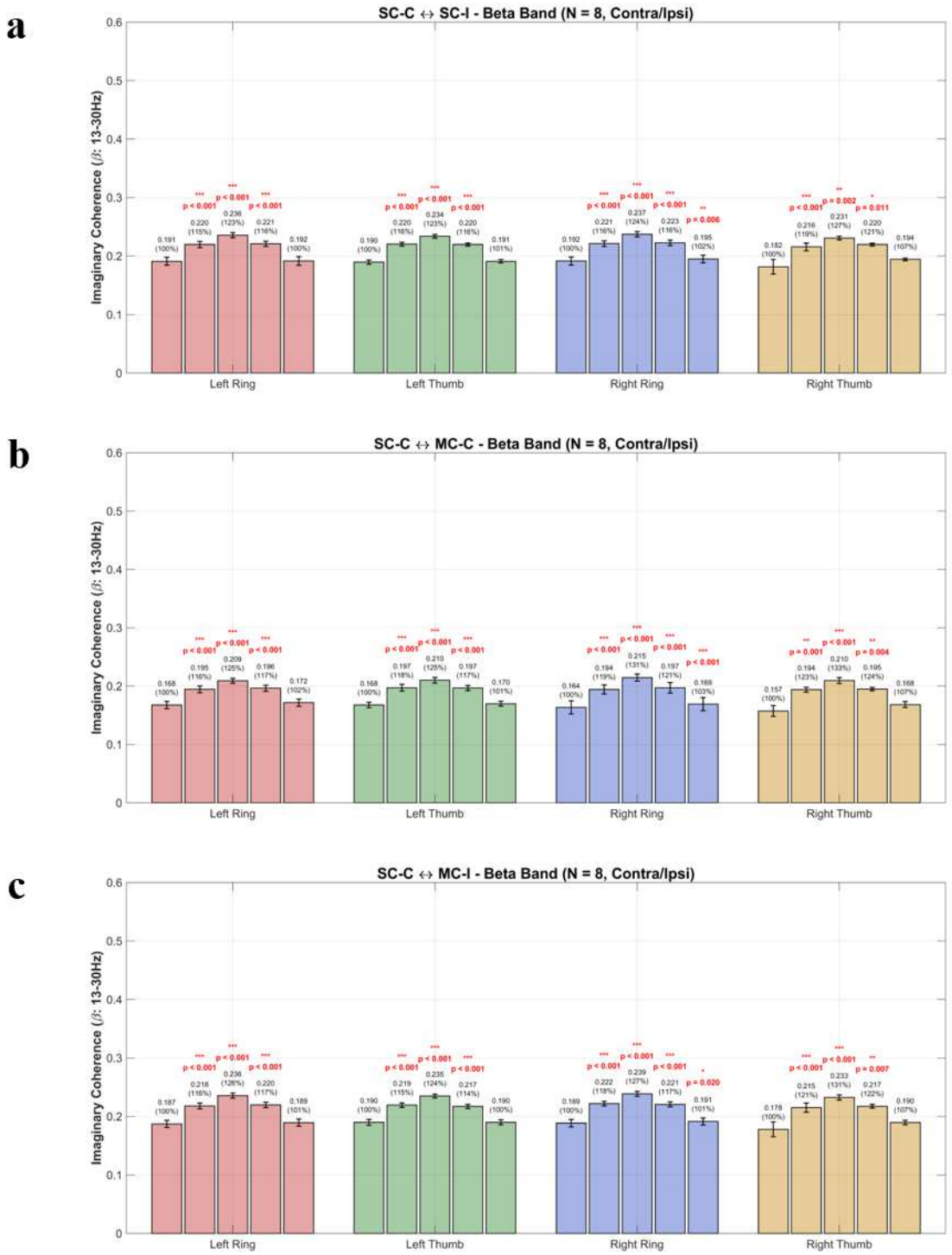


Fig. 11. Changes in imaginary coherence between the contralateral somatosensory cortex (SC-C) and three cortical regions in the beta band (13–40 Hz) before and after TENS. (a) SC-C ↔ SC-I; (b) SC-C ↔ MC-C; (c) SC-C ↔ MC-I.

DISCUSSION

This study combined psychophysical testing and MEG to characterize digit-specific electrotactile sensation and its cortical substrates during transcutaneous electrical stimulation. Three main findings emerged. First, electrotactile perception thresholds differed across digits, whereas Weber fractions did not show significant hand- or digit-dependent effects. Second, TENS consistently elicited an early somatosensory response, but group-level early-response peak latency and amplitude did not differ significantly between the thumb and ring finger or between the two hands. Third, TENS induced time- and frequency-dependent modulation of sensorimotor cortical connectivity, with the strongest connectivity increase occurring 100–200 ms after stimulation and with alpha-band coherence exceeding beta-band coherence. These findings extend previous work on artificial tactile feedback and TENS-based sensory substitution by linking digit-level psychophysical thresholds with MEG-derived cortical activation and functional connectivity measures [12–16,20,21,23,24].

DIGIT-SPECIFIC ELECTROTACTILE PERCEPTION

The psychophysical results indicate that perception thresholds, rather than Weber fractions, were the more sensitive behavioural index of digit-specific electrotactile sensation in this cohort. The right thumb showed higher thresholds than the ring fingers, while Weber fractions remained statistically comparable across digits. This dissociation suggests that the minimal current required to detect stimulation and the ability to discriminate suprathreshold intensity differences may reflect partially distinct sensory processes. Such a distinction is consistent with psychophysical theory, in which detection thresholds and Weber fractions capture different aspects of sensory performance [25].

In right-handed participants, the thumb is frequently engaged in grasping, object manipulation, touchscreen interaction, and fine motor control. Higher thresholds in the thumb may therefore reflect long-term use-dependent adaptation of tactile processing. This interpretation is compatible with evidence that handedness and upper-limb asymmetry influence sensorimotor performance [30], and that repeated sensory use can reshape cortical processing and somatotopic representations [31,32]. However, this explanation should be considered cautiously. The present study did not directly

quantify daily digit use or peripheral nerve properties, and the hand main effect reached only a near-significant level. Thus, the behavioural findings are best interpreted as evidence for digit-specific variability in electrotactile detection sensitivity, with the right thumb showing the clearest threshold elevation relative to the ring fingers.

The absence of significant differences in Weber fractions is also informative. Although detection sensitivity differed across digits, once stimulation was perceived, the relative ability to discriminate intensity increments appeared broadly preserved. This pattern may be relevant for artificial tactile feedback design: digit-specific threshold calibration may be necessary to ensure detectability, whereas a shared intensity-scaling strategy may still be feasible for suprathreshold discrimination. This interpretation aligns with prior studies showing that non-invasive electrotactile feedback can support artificial tactile perception and sensory substitution when stimulation parameters are individually calibrated [14–16,21,23,24]. Future studies with larger samples should test this possibility by directly comparing threshold-normalized stimulation and perceptual scaling across digits.

CORTICAL RESPONSES TO DIGIT-SPECIFIC TENS

MEG recordings showed that TENS reliably evoked an early-response peak at approximately 35–70 ms after stimulation. This latency range is consistent with early somatosensory cortical processing and supports the feasibility of using finger TENS to evoke measurable cortical responses. Previous MEG studies have demonstrated that somatosensory stimulation and artificial sensory experience can modulate cortical neuromagnetic responses [18–20,33]. However, in the present dataset, early-response peak latency and amplitude did not show significant main effects of hand or digit, nor significant hand × digit interactions. Therefore, the MEG results do not support a robust group-level difference in early evoked response timing or magnitude between thumb and ring-finger stimulation under the present sample size.

The correlation analyses further suggest that behavioural thresholds, early-response peak latency and amplitude were not strongly coupled at the pooled level. Across all stimulation sites, no significant linear or monotonic associations were observed among these measures. This indicates that digit-specific detection thresholds cannot be directly inferred from early-response peak latency or amplitude alone. Instead, electrotactile perception likely depends on a combination of peripheral excitability, stimulus-site properties, cortical representation, and distributed network-level processing. This interpretation is consistent with studies emphasizing that tactile perception and sensorimotor control arise from interactions between peripheral feedback and cortical processing rather than from a single isolated neural marker [10,11].

At the same time, the right ring finger showed a site-specific negative correlation between early-response peak latency and amplitude. This finding suggests that, for some stimulation sites, faster cortical responses may be accompanied by stronger evoked activity. Because this effect was not observed for the other digits and was based on a modest sample, it should be regarded as exploratory. Nevertheless, it highlights the potential value of analysing digit-specific neurophysiological signatures rather than averaging across fingers.

Source localization provided additional spatial information. Fixed-dipole modelling showed that responses were localized predominantly to regions contralateral to the stimulated digits. Compared with the ring finger, the thumb, which had higher behavioural thresholds, showed response locations closer to the superficial region of the tactile cortex. Moving-dipole modelling further showed that source locations evolved over time after stimulation, with most dipoles clustering around the central sulcus and postcentral gyrus and then shifting toward deeper regions around 60 ms. These findings support the view that TENS-evoked cortical activity is both digit-specific and temporally dynamic, consistent with the broader concept of use-dependent cortical plasticity in somatosensory maps [31,32].

SENSORIMOTOR CONNECTIVITY INDUCED BY TENS

The functional connectivity results suggest that finger TENS transiently enhances coupling within the sensorimotor network. Across stimulated digits, imaginary coherence increased after stimulation, with the largest average increase observed during the 100–200 ms post-stimulation window. This temporal profile indicates that the strongest network-level modulation occurred after the early-response peak, suggesting a progression from early somatosensory activation to subsequent sensorimotor network engagement. Imaginary coherence is appropriate for this analysis because it reduces the influence of volume conduction and captures phase-lagged inter-regional coupling [26–28].

The right ring finger showed the slowest recovery toward baseline, with connectivity remaining significantly different from baseline during the 300–400 ms window, particularly for SC-C ↔ SC-I and SC-C ↔ MC-C pathways. This prolonged modulation is consistent with the relatively delayed early-response peak characteristics observed for the same digit and may reflect site-specific differences in sensorimotor integration. However, because the current study was conducted in healthy young adults, this result should be interpreted as a physiological observation rather than direct evidence of clinical efficacy.

Frequency-dependent effects were also observed. Imaginary coherence values were consistently higher in the alpha band than in the beta band across pathways, digits, and time windows. This finding suggests that alpha-band interactions may be particularly sensitive to TENS-induced somatosensory network modulation in the present paradigm. Sensorimotor alpha- and beta-band oscillations are known to be modulated during tactile attention and upcoming tactile events [29]. The stable pathway hierarchy, SC-C ↔ SC-I > SC-C ↔ MC-C > SC-C ↔ MC-I, further indicates that TENS primarily strengthened somatosensory-to-somatosensory coupling, followed by coupling between somatosensory and motor cortices.

These network-level findings may have implications for sensory-guided motor rehabilitation. Somatosensory deficits after stroke are common and are associated with upper-limb impairment, activity limitations, and poorer rehabilitation response [4–9,17]. Connectivity-based frameworks further suggest that recovery after stroke depends not only on local cortical excitability but also on reorganization of distributed sensorimotor networks [34]. By enhancing phase-lagged connectivity between somatosensory and motor regions, digit-specific TENS may provide a non-invasive strategy for engaging sensorimotor circuits. Nevertheless, the present data were obtained from healthy participants and did not include motor outcome measures. Therefore, the translational relevance of these connectivity changes remains to be tested in clinical populations, despite emerging evidence that TENS may improve upper-limb function after stroke [35,36].

LIMITATIONS AND FUTURE DIRECTIONS

Several limitations should be considered. First, the sample size was modest, particularly for the MEG experiment and correlation analyses. This limited statistical power may partly explain why several MEG effects did not reach significance despite observable trends. Second, all participants were young, healthy, and right-handed. The findings may not generalize to older adults, left-handed individuals, or patients with neurological impairment. Third, daily digit-use frequency, peripheral nerve excitability, skin impedance, and individual anatomical variability were not directly quantified, limiting mechanistic interpretation of digit-specific threshold differences. Fourth, the study focused on immediate cortical responses and short post-stimulation time windows. It did not assess whether repeated TENS produces durable changes in tactile perception, cortical excitability, or motor function. Fifth, although imaginary coherence reduces the influence of volume conduction, connectivity estimates from MEG remain dependent on source modelling choices and region-of-interest definitions [26–28].

Future work should include larger and more diverse cohorts, quantify individual digit-use habits and peripheral sensory properties, and combine MEG with behavioural motor outcomes. In clinical populations such as stroke survivors, future studies should test whether digit-specific threshold calibration and TENS-induced sensorimotor connectivity changes predict improvements in tactile feedback, fine motor control, or rehabilitation outcomes [4–9,17,34,35,36].

CONCLUSION

The present study systematically investigated finger electrotactile sensation and its underlying neural mechanisms through combined psychophysical measurements and MEG recordings. Three key findings were summarized, carrying important implications for clinical sensorimotor rehabilitation.

Psychophysical testing showed that electrotactile perception thresholds varied across digits in healthy right-handed adults, whereas Weber fractions did not differ significantly across hands or digits. The right thumb required higher stimulation intensity than the ring fingers, indicating higher detection thresholds at this frequently used digit. These findings suggest that digit-specific threshold calibration is necessary for reliable artificial tactile feedback and for individualized TENS protocols [14–16,21,23–25].

MEG recordings further demonstrated that finger TENS consistently evoked an early somatosensory response and produced cortical activation patterns predominantly contralateral to the stimulated digits. Although group-level latency and amplitude did not differ significantly across stimulation sites, source localization and site-specific correlation analyses suggested that digit stimulation may have distinct spatial and temporal cortical signatures. These results support the use of MEG as a non-invasive tool for characterizing cortical responses to artificial tactile stimulation [18–20,22,33].

Functional connectivity analyses showed that TENS transiently enhanced sensorimotor cortical coupling, with the strongest modulation occurring during the 100–200 ms post-stimulation window. Connectivity changes were more prominent in the alpha band than in the beta band and followed a stable pathway hierarchy, with the strongest coupling between contralateral and ipsilateral somatosensory cortices. These findings indicate that digit-specific TENS engages not only early somatosensory responses but also broader phase-lagged sensorimotor networks [26–28,29].

Overall, this study provides a normative psychophysical and MEG-based framework for evaluating digit-specific electrotactile feedback in healthy adults. By linking behavioural thresholds, cortical source patterns, and sensorimotor

connectivity, the present work establishes a methodological foundation for future studies of artificial tactile restoration. Clinical studies in stroke survivors are needed to determine whether individualized TENS can improve impaired tactile processing, strengthen disrupted sensorimotor connectivity, and contribute to fine motor recovery [4–9,17,34,35,36].

LIST OF ABBREVIATIONS

TENS: Transcutaneous Electrical Nerve Stimulation

MEG: Magnetoencephalography

SEFs: Somatosensory Evoked Fields

JND: Just-Noticeable Difference

ANOVA: Analysis of Variance

HSD: Honestly Significant Difference

MRI: Magnetic Resonance Imaging

DALYs: Disability-Adjusted Life-Years

BCI: Brain-Computer Interface

ERF: Event-Related Field

GOF: Goodness-of-Fit

US: United States

GDP: Gross Domestic Product

DECLARATIONS

ETHICS APPROVAL AND CONSENT TO PARTICIPATE

This study involving human participants was reviewed and approved by the institutional review boards of Shanghai Jiao Tong University (No. B20230256) and West China Hospital, Sichuan University (No. 2024 Review (607) & (644)). All participants provided written informed consent prior to participation, in accordance with the Declaration of Helsinki. The consent process included detailed explanation of the study's purpose, procedures, potential risks, and the right to withdraw at any time without penalty.

CONSENT FOR PUBLICATION

This manuscript does not contain any individual person's identifiable data (including individual details, images, or videos), so consent for publication is not applicable.

AVAILABILITY OF DATA AND MATERIALS

The datasets generated and/or analysed during the current study contain sensitive human neurophysiological and identifiable information. Due to ethical restrictions and privacy regulations approved by the Institutional Review Board of West China Hospital, Sichuan University, the datasets are not publicly available. Requests for qualified access to anonymized data will be considered by the corresponding author (Xiaohong Sui; E-mail: suixhong@sjtu.edu.cn) upon reasonable request and with appropriate ethical approvals.

COMPETING INTERESTS

The authors declare that they have no competing interests.

FUNDING

This research is supported by the National Key Research and Development Program of China (Nos. 2022YFC3601103, 2024YFE0200900), the National Natural Science Foundation of China (No. 62176158), and the STAR Project of Shanghai Jiao Tong University (20220103). The funders had no role in the conceptualization, design, data collection, analysis, decision to publish, or preparation of the manuscript.

AUTHORS' CONTRIBUTIONS

XHS contributed to the conception and design of the study; JTL, DKY, and XHS contributed to data acquisition and analysis, paper drafting and revision. JTL, DKY, YGH, JBH, JH, NJ, XLG and YC contributed to the resources and paper revision. All authors read and approved the final manuscript.

ACKNOWLEDGEMENTS

The authors would like to thank all participants who volunteered for this study.

POTENTIAL CONFLICTS OF INTEREST

The authors have no conflicts of interest to report.

DATA AVAILABILITY STATEMENT

The data that support the findings of this study contain sensitive human neurophysiological and identifiable information. Due to ethical restrictions and privacy regulations approved by the Institutional Review Board of West China Hospital, Sichuan University, the datasets are not publicly available. Requests for qualified access to anonymized data will be considered by the corresponding author upon reasonable request and with appropriate ethical approvals.

REFERENCES

1. Feigin VL, Brainin M, Norrving B, et al. World Stroke Organization (WSO): Global Stroke Fact Sheet 2022. International Journal of Stroke 2022;17(1):18-29.
2. Wang Y, Li Z, Gu H, et al. China stroke report 2020 (Chinese version). Zhongguo Cuzhong Zazhi 2022;17(5):433-447. (in Chinese)
3. Martin SS, Aday AW, Almarzooq ZI, et al. 2024 Heart Disease and Stroke Statistics: A Report of US and Global Data From the American Heart Association. Circulation 2024;149(8):e347-e913.
4. Kessner SS, Schlemm E, Cheng B, et al. Somatosensory Deficits After Ischemic Stroke. Stroke 2019;50(5):1116-1123.
5. Borstad AL, Nichols-Larsen DS. Assessing and treating higher level somatosensory impairments post stroke. Topics in Stroke Rehabilitation 2014;21(4):290-295.

6. Doyle SD, Bennett S, Dudgeon B. Upper limb post-stroke sensory impairments: the survivor's experience. Disability and Rehabilitation 2014;36(12):993-1000.

7. Meyer S, Karttunen AH, Thijs V, et al. How do somatosensory deficits in the arm and hand relate to upper limb impairment, activity, and participation problems after stroke? A systematic review. Physical Therapy 2014;94(9):1220-1231.

8. Turville ML, Matyas TA, Blennerhassett JM, et al. Initial severity of somatosensory impairment influences response to upper limb sensory retraining post-stroke. NeuroRehabilitation 2018;43(4):413-423.

9. Pillette L, Lotte F, N'Kaoua B, et al. Why we should systematically assess, control and report somatosensory impairments in BCI-based motor rehabilitation after stroke studies. NeuroImage: Clinical 2020;28:102417.

10. Li R, Huang ZC, Cui HY, et al. Utility of somatosensory and motor-evoked potentials in reflecting gross and fine motor functions after unilateral cervical spinal cord contusion injury. Neural Regeneration Research 2021;16(7):1323-1330.

11. Johansson R, Flanagan J. Tactile sensory control of object manipulation in humans. In: Basbaum AI, Kaneko A, Shepherd GM, et al, eds. Senses: A Comprehensive Reference. New York, NY: Academic Press; 2008:67-86.

12. Ge Y, Ye S, Zhu K, et al. Mediating different-diameter Aβ nerve fibers using a biomimetic 3D TENS computational model. Journal of Neuroscience Methods 2020;346:108891.

13. Zhu K, Li L, Wei X, et al. A 3D Computational Model of Transcutaneous Electrical Nerve Stimulation for Estimating Aβ Tactile Nerve Fiber Excitability. Frontiers in Neuroscience 2017;11:250.

14. D'Alonzo M, Dosen S, Cipriani C, et al. HyVE: hybrid vibro-electrotactile stimulation for sensory feedback and substitution in rehabilitation. IEEE Transactions on Neural Systems and Rehabilitation Engineering 2014;22(2):290-301.

15. Yoshimoto S, Kuroda Y, Imura M, et al. Material Roughness Modulation via Electrotactile Augmentation. IEEE Transactions on Haptics 2015;8(2):199-208.

16. Scarpelli A, Demofonti A, Cordella F, et al. Eliciting Force and Slippage in Upper Limb Amputees Through Transcutaneous Electrical Nerve Stimulation (TENS). IEEE Transactions on Neural Systems and Rehabilitation Engineering 2024;32:3006-3017.

17. Bowden JL, Lin GG, McNulty PA. The Prevalence and Magnitude of Impaired Cutaneous Sensation across the Hand in the Chronic Period Post-Stroke. PLoS One 2014;9(8):e104153.

18. Andrade GN, Butler JS, Peters GA, et al. Atypical visual and somatosensory adaptation in schizophrenia-spectrum disorders. Translational Psychiatry 2016;6(5):e804.

19. Daskalakis AA, Zomorrodi R, Blumberger DM, et al. Evidence for prefrontal cortex hypofunctioning in schizophrenia through somatosensory evoked potentials. Schizophrenia Research 2020;215:197-203.

20. Isabella SL, D'Alonzo M, Mioli A, et al. Artificial embodiment displaces cortical neuromagnetic somatosensory responses. Scientific Reports 2024;14(1):22279.

21. Hao M, Chou CH, Zhang J, et al. Restoring Finger-Specific Sensory Feedback for Transradial Amputees via Non-Invasive Evoked Tactile Sensation. IEEE Open Journal of Engineering in Medicine and Biology 2020;1:98-107.

22. Gallien P, Aghulon C, Durufle A, et al. Magnetoencephalography in stroke: a 1-year follow-up study. European Journal of Neurology 2003;10(4):373-382.

23. Li M, Zhang D, Chen Y, et al. Discrimination and Recognition of Phantom Finger Sensation Through Transcutaneous Electrical Nerve Stimulation. Frontiers in Neuroscience 2018;12:283.

24. Graczyk EL, et al. The neural basis of perceived intensity in natural and artificial touch. Science Translational Medicine 2016;8(362):362ra142.

25. Ekman G. Weber's law and related functions. Journal of Psychology 1959;47(2):343-352.

26. Lowet E, Roberts MJ, Bonizzi P, et al. Quantifying Neural Oscillatory Synchronization: A Comparison between Spectral Coherence and Phase-Locking Value Approaches. PLoS One 2016;11(1):e0146443.

27. Le Van Quyen M, Foucher J, Lachaux J, et al. Comparison of Hilbert transform and wavelet methods for the analysis of neuronal synchrony. Journal of Neuroscience Methods 2001;111(2):83-98.

28. Mima T, Matsuoka T, Hallett M. Functional coupling of human right and left cortical motor areas demonstrated with partial coherence analysis. Neuroscience Letters 2000;287(2):93-96.

29. Van Ede F, De Lange F, Jensen O, et al. Orienting Attention to an Upcoming Tactile Event Involves a Spatially and Temporally Specific Modulation of Sensorimotor Alpha- and Beta-Band Oscillations. The Journal of Neuroscience 2011;31(6):2016-2024.

30. Goble DJ, Brown SH. The biological and behavioral basis of upper limb asymmetries in sensorimotor performance. Neuroscience and Biobehavioral Reviews 2008;32(3):598-610.

31. Buonomano DV, Merzenich MM. Cortical plasticity: from synapses to maps. Annual Review of Neuroscience 1998;21(1):149-186.

32. Gindrat AD, Chytiris M, Balerna M, et al. Use-Dependent Cortical Processing from Fingertips in Touchscreen Phone Users. Current Biology 2015;25(1):109-116.

33. Pihko E, Nangini C, Jousmäki V, et al. Observing touch activates human primary somatosensory cortex. European Journal of Neuroscience 2010;31(10):1836-1843.

34. Grefkes C, Fink GR. Connectivity-based approaches in stroke and recovery of function. The Lancet Neurology 2014;13(2):206-216.

35. Song C, Wu W, Feng N, et al. Rehabilitative effects of Transcutaneous Electric Nerve Stimulation on limb function in stroke patients: a systematic review and meta-analysis. Disability and Rehabilitation 2025;47(18):4645-4652.

36. Alashram AR. Effects of transcutaneous electrical nerve stimulation on upper limb recovery in stroke survivors: A systematic review and meta-analysis of randomized controlled trials. Journal of Hand Therapy 2026;39(1):109-119.

FIGURE LEGENDS

Figure.1 Schematic of the psychophysical experiment under TENS. a. Experimental setup; b. Diagram of electrical stimulus parameters, where pulse amplitude represents stimulation intensity, with a constant pulse frequency of 50 Hz and pulse width of 200 μs; c. Two successive observation intervals per trial, containing one inactive null stimulus and one active electrical stimulus; d. Tactile detection threshold estimated via psychometric function fitting, defined at 75% correct discrimination accuracy; e. Protocols of two experiments: detection threshold measurement (top) and just noticeable difference discrimination (bottom). Pulse amplitude (PA) was modulated at fixed PF = 50 Hz and PW = 200 μs. Stimulation trials were pseudo-randomized within each block, with an inter-trial interval of approximately 2 s.

Figure. 2. MEG data processing pipeline

Figure. 3 Repeated-measures ANOVA results for electrotactile perception thresholds. (a) Main effect of hand; (b) main effect of digit; (c) hand × digit interaction.

Figure. 4 Repeated-measures ANOVA results for Weber fractions. (a) Main effect of hand; (b) main effect of digit; (c) hand × digit interaction.

Figure. 5 Somatosensory evoked fields induced by left-hand electrical stimulation in Participant 1. (a) Temporal dynamics of SEFs across the 306-channel sensor array; (b) spatial topography of the peak SEF response in representative channels.

Figure.6 Repeated-measures ANOVA results for early-response peak. (a) early-response peak latency; (b) early-response peak amplitude.

Figure.7 Scatter plots and regression analyses. (a) Latency versus amplitude; (b) latency versus threshold; (c) amplitude versus threshold.

Figure.8 Correlation matrices for latency, amplitude, and electrotactile threshold. (a) Pearson correlation matrix of 12 variables (4 stimulation sites × 3 measures), with correlation coefficients and significance levels shown in the lower triangle (*p < 0.05, **p < 0.01, ***p < 0.001); black lines separate latency, amplitude, and threshold modules. (b) Aggregated correlation matrix among the three measures.

Figure.9 Cortical source locations reconstructed using fixed- and moving-dipole models during digit transcutaneous electrical stimulation. (a) Fixed dipole source results for Participant 1; (b) Temporal dynamics of moving dipole sources in Participant 1 elicited by left ring finger stimulation.

Figure.10 Changes in imaginary coherence between the contralateral somatosensory cortex (SC-C) and three cortical regions in the alpha band (8–13 Hz) before and after TENS. (a) SC-C ↔ SC-I; (b) SC-C ↔ MC-C; (c) SC-C ↔ MC-I.

Figure.11 Changes in imaginary coherence between the contralateral somatosensory cortex (SC-C) and three cortical regions in the beta band (13–40 Hz) before and after TENS. (a) SC-C ↔ SC-I; (b) SC-C ↔ MC-C; (c) SC-C ↔ MC-I.

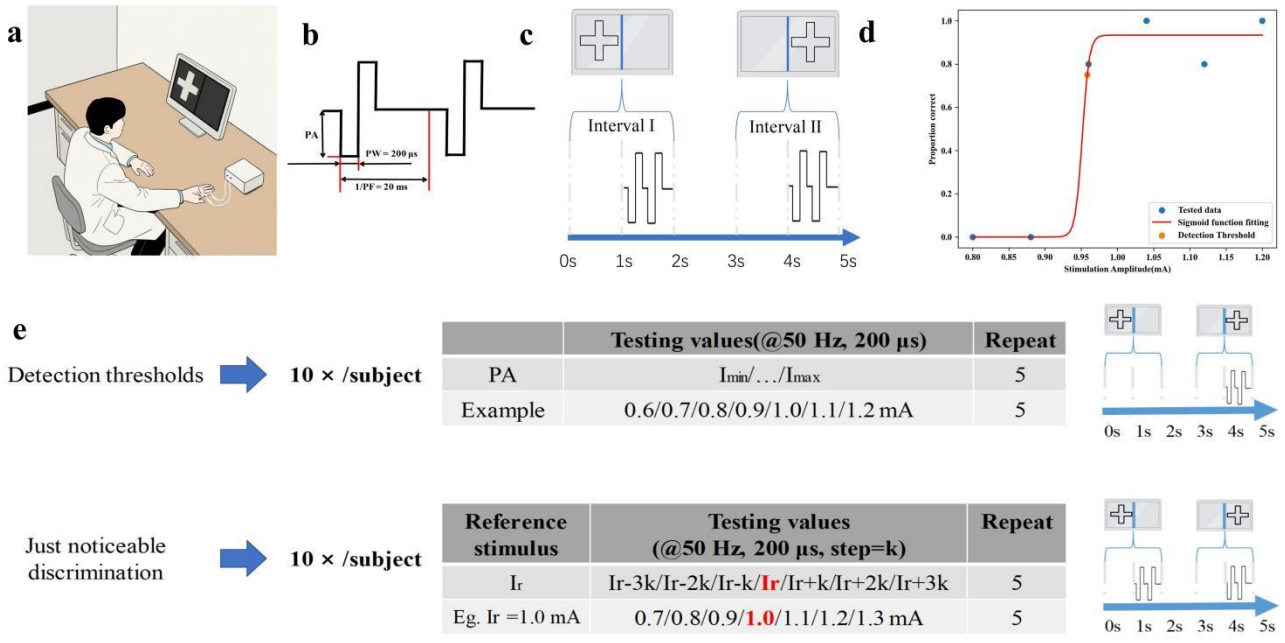


Figure 1

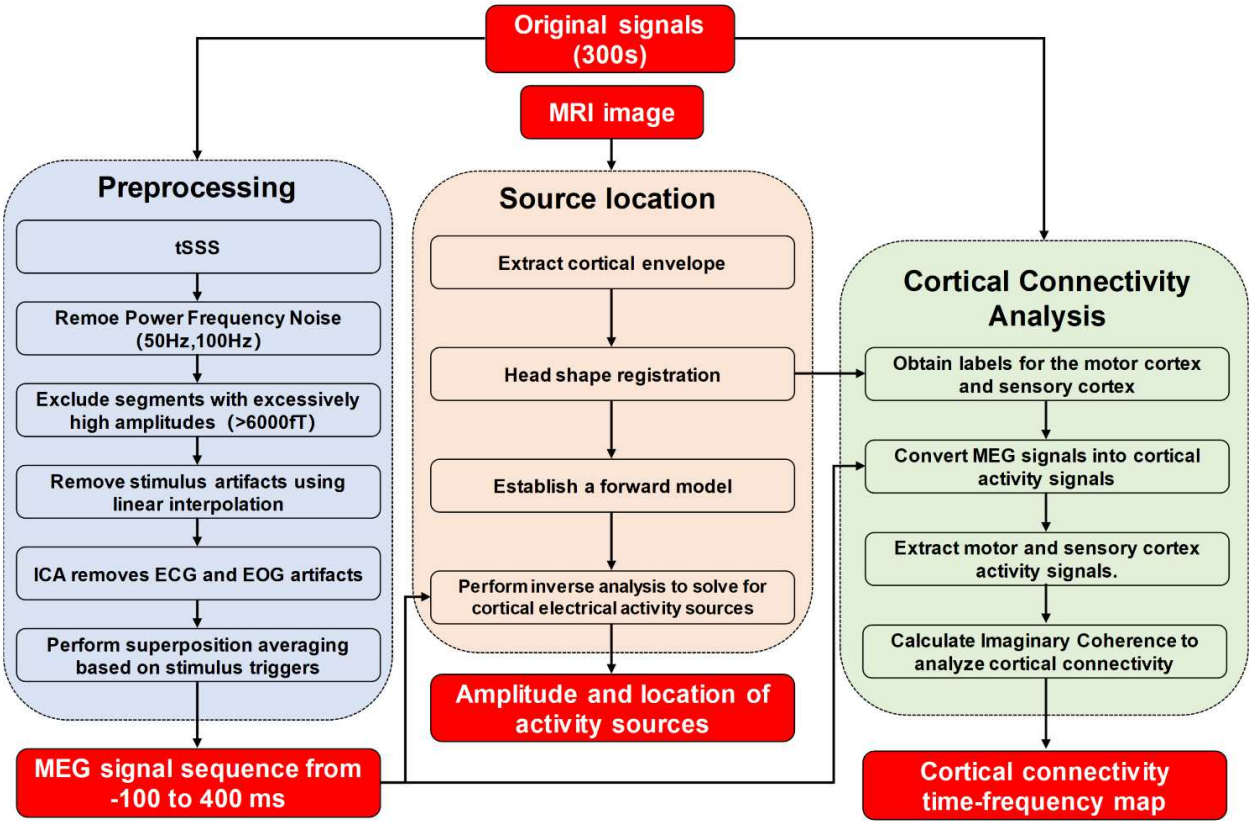

Original signals (300s)
MRI image
Preprocessing
tSSS
Remoe Power Frequency Noise (50Hz,100Hz)
Exclude segments with excessively high amplitudes (>6000fT)
Remove stimulus artifacts using linear interpolation
ICA removes ECG and EOG artifacts
Perform superposition averaging based on stimulus triggers
MEG signal sequence from -100 to 400 ms
Source location
Extract cortical envelope
Head shape registration
Establish a forward model
Perform inverse analysis to solve for cortical electrical activity sources
Amplitude and location of activity sources
Cortical Connectivity Analysis
Obtain labels for the motor cortex and sensory cortex
Convert MEG signals into cortical activity signals
Extract motor and sensory cortex activity signals.
Calculate Imaginary Coherence to analyze cortical connectivity
Cortical connectivity time-frequency map

Figure 2

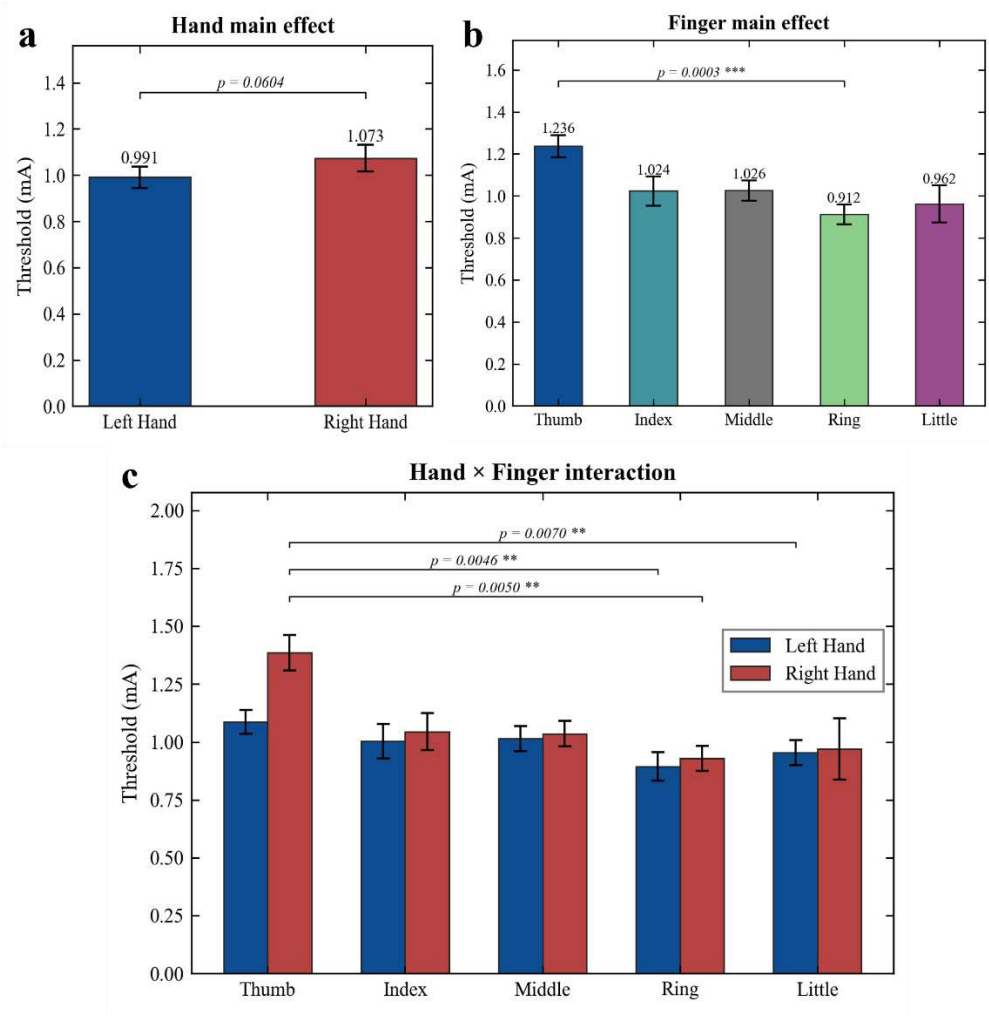

a
Hand main effect
p = 0.0604
0.991
1.073
Threshold (mA)
Left Hand
Right Hand
b
Finger main effect
p = 0.0003 ***
1.236
1.024
1.026
0.912
0.962
Threshold (mA)
Thumb
Index
Middle
Ring
Little
c
Hand × Finger interaction
p = 0.0070 **
p = 0.0046 **
p = 0.0050 **
Left Hand
Right Hand
Threshold (mA)
Thumb
Index
Middle
Ring
Little

Figure 3

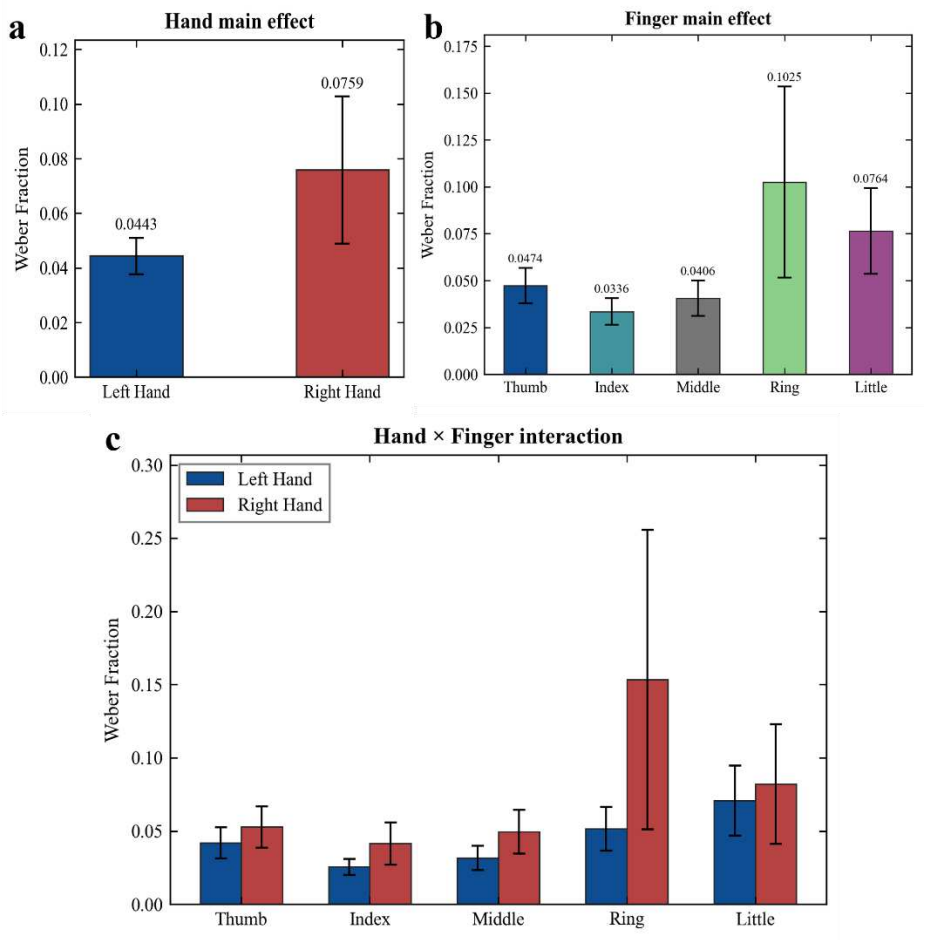


Figure 4

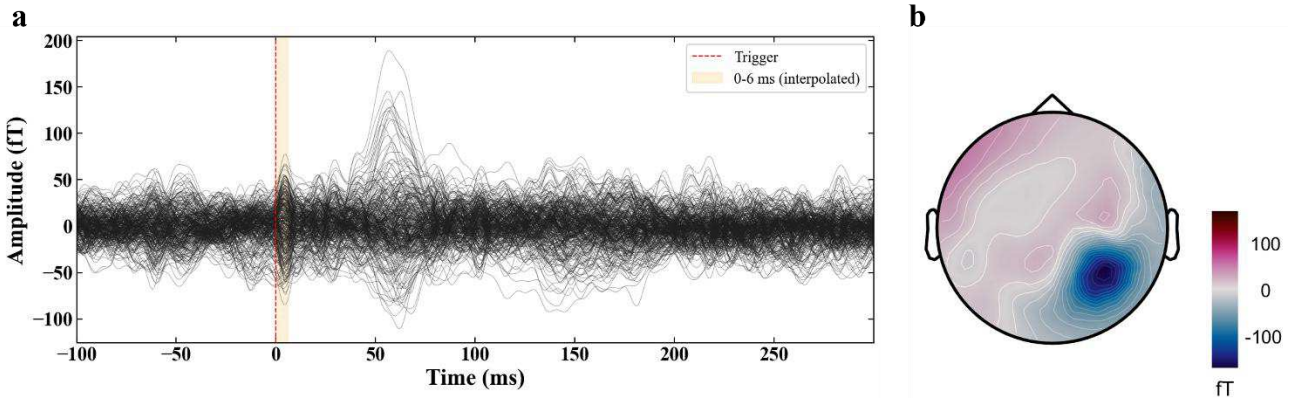


Figure 5

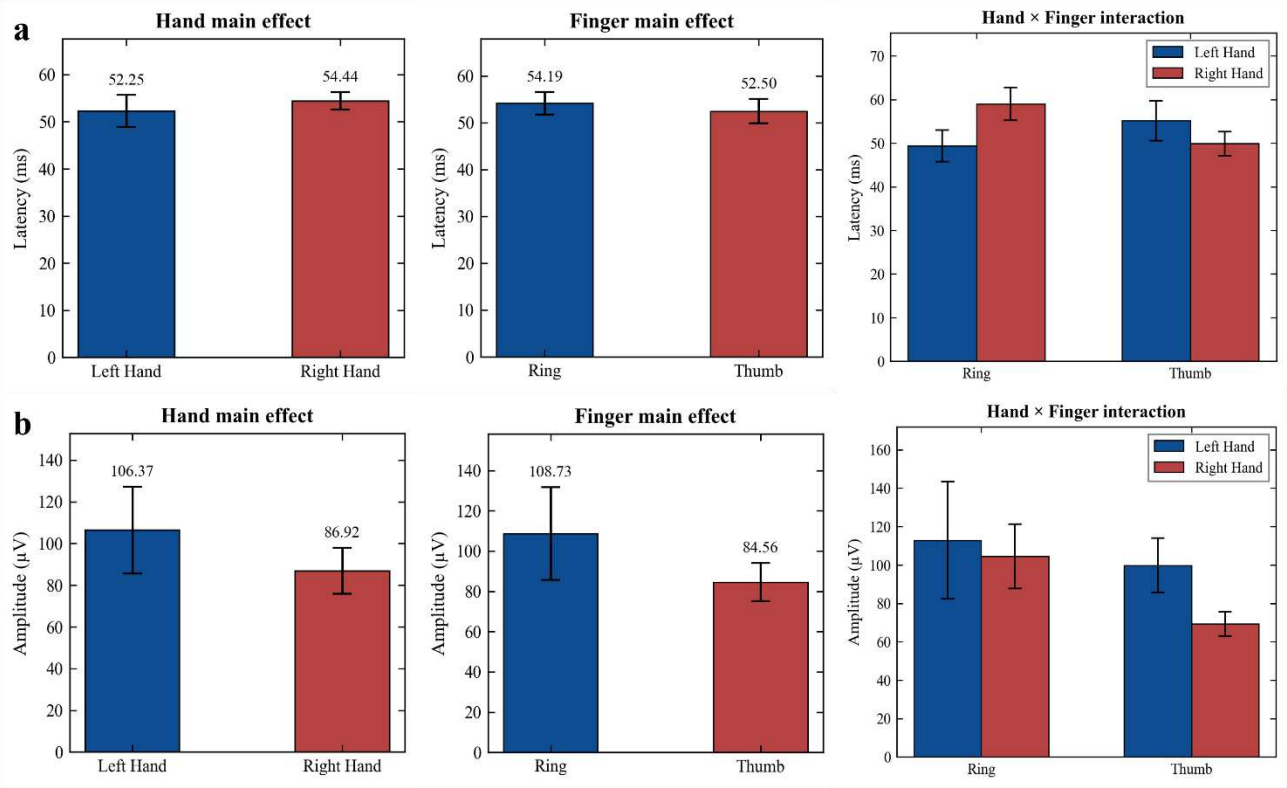


Figure 6

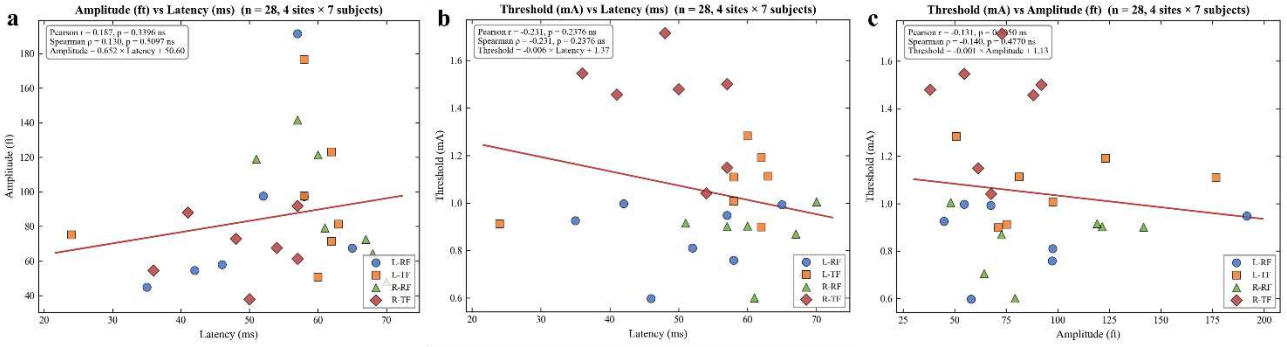


Figure 7

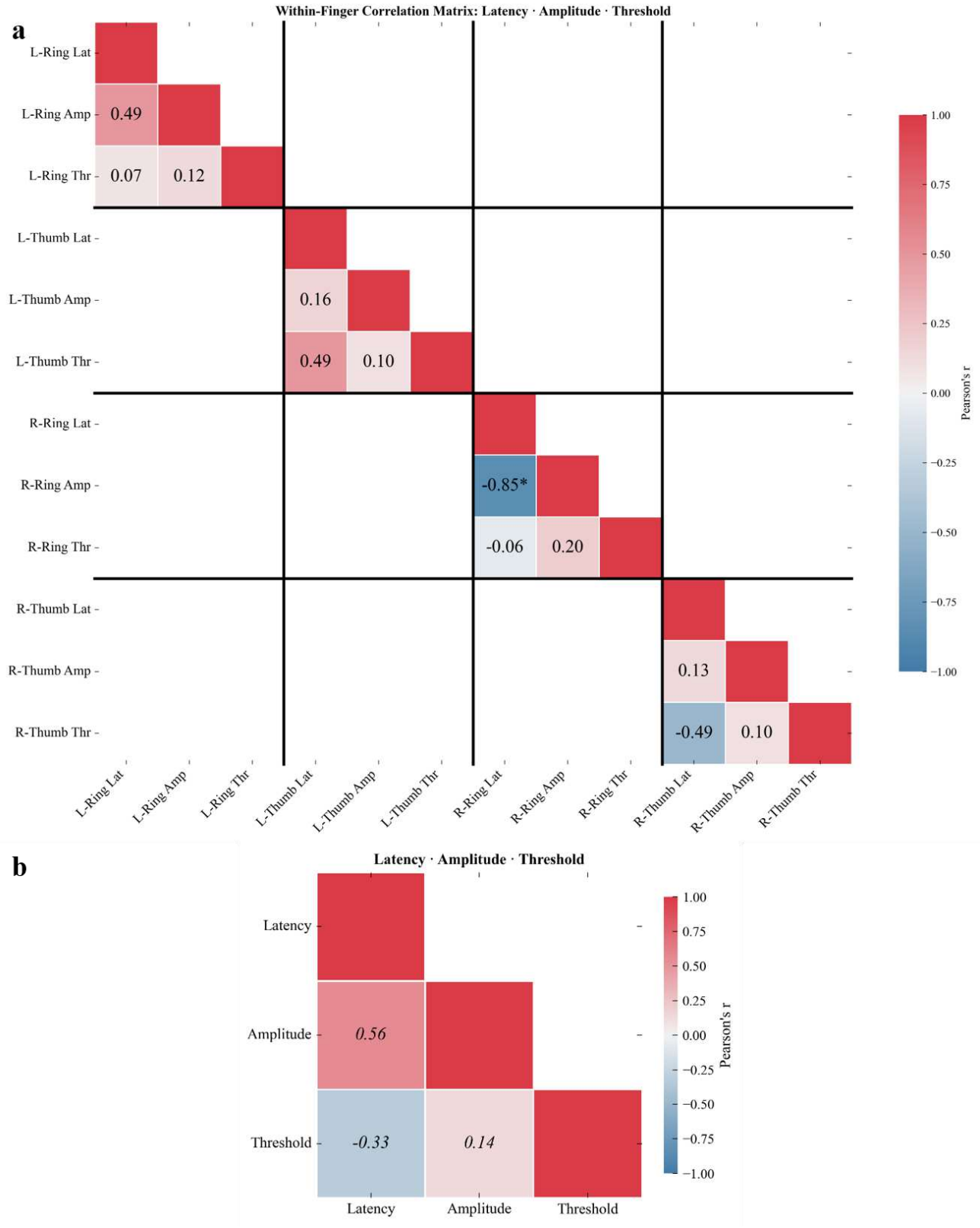

a
Within-Finger Correlation Matrix: Latency · Amplitude · Threshold
L-Ring Lat
L-Ring Amp
L-Ring Thr
L-Thumb Lat
L-Thumb Amp
L-Thumb Thr
R-Ring Lat
R-Ring Amp
R-Ring Thr
R-Thumb Lat
R-Thumb Amp
R-Thumb Thr
0.49
0.07
0.12
0.16
0.49
0.10
-0.85*
-0.06
0.20
0.13
-0.49
0.10
1.00
0.75
0.50
0.25
0.00
−0.25
−0.50
−0.75
−1.00
Pearson's r
b
Latency · Amplitude · Threshold
Latency
Amplitude
Threshold
0.56
-0.33
0.14
1.00
0.75
0.50
0.25
0.00
−0.25
−0.50
−0.75
−1.00
Pearson's r

Figure 8

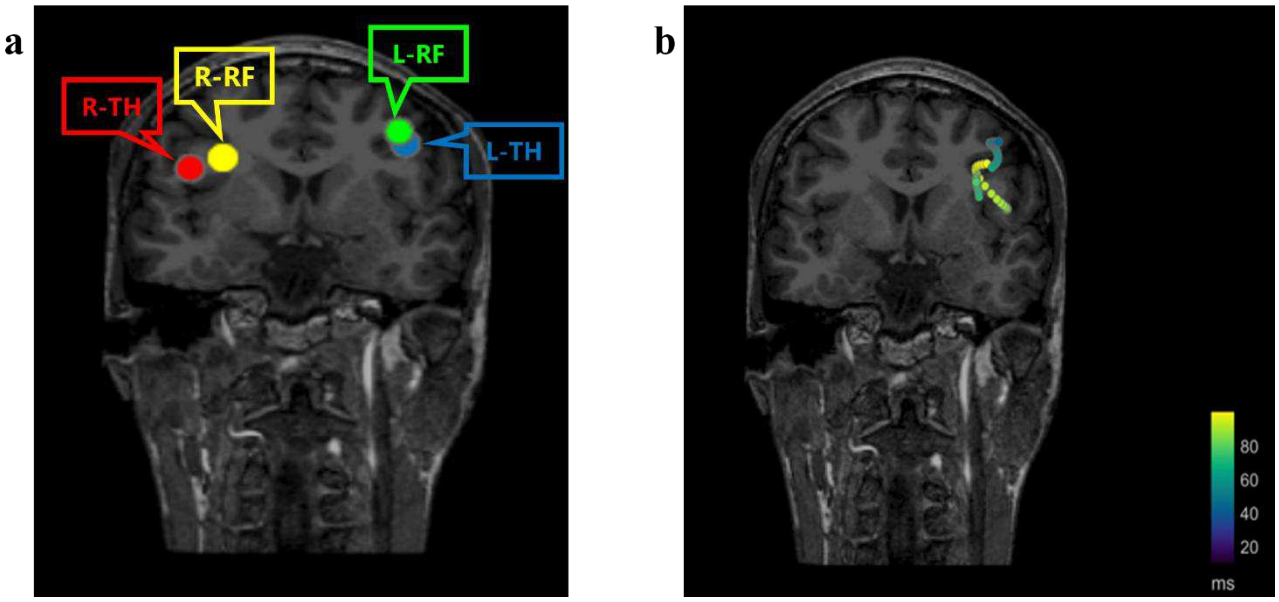


Figure 9

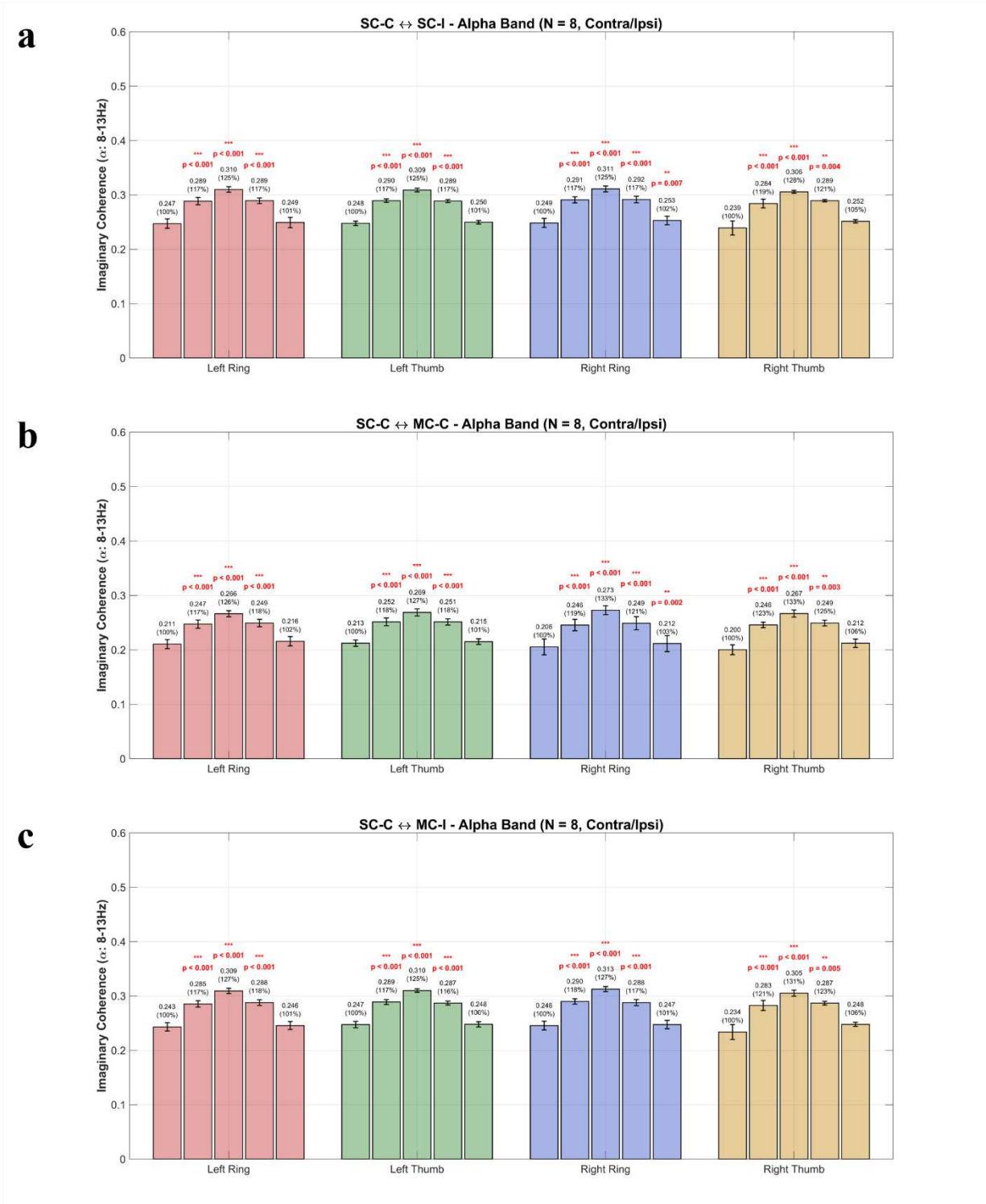

a
SC-C ↔ SC-I - Alpha Band (N = 8, Contra/Ipsi)
b
SC-C ↔ MC-C - Alpha Band (N = 8, Contra/Ipsi)
c
SC-C ↔ MC-I - Alpha Band (N = 8, Contra/Ipsi)
Imaginary Coherence (α: 8-13Hz)
Left Ring
Left Thumb
Right Ring
Right Thumb

Figure 10

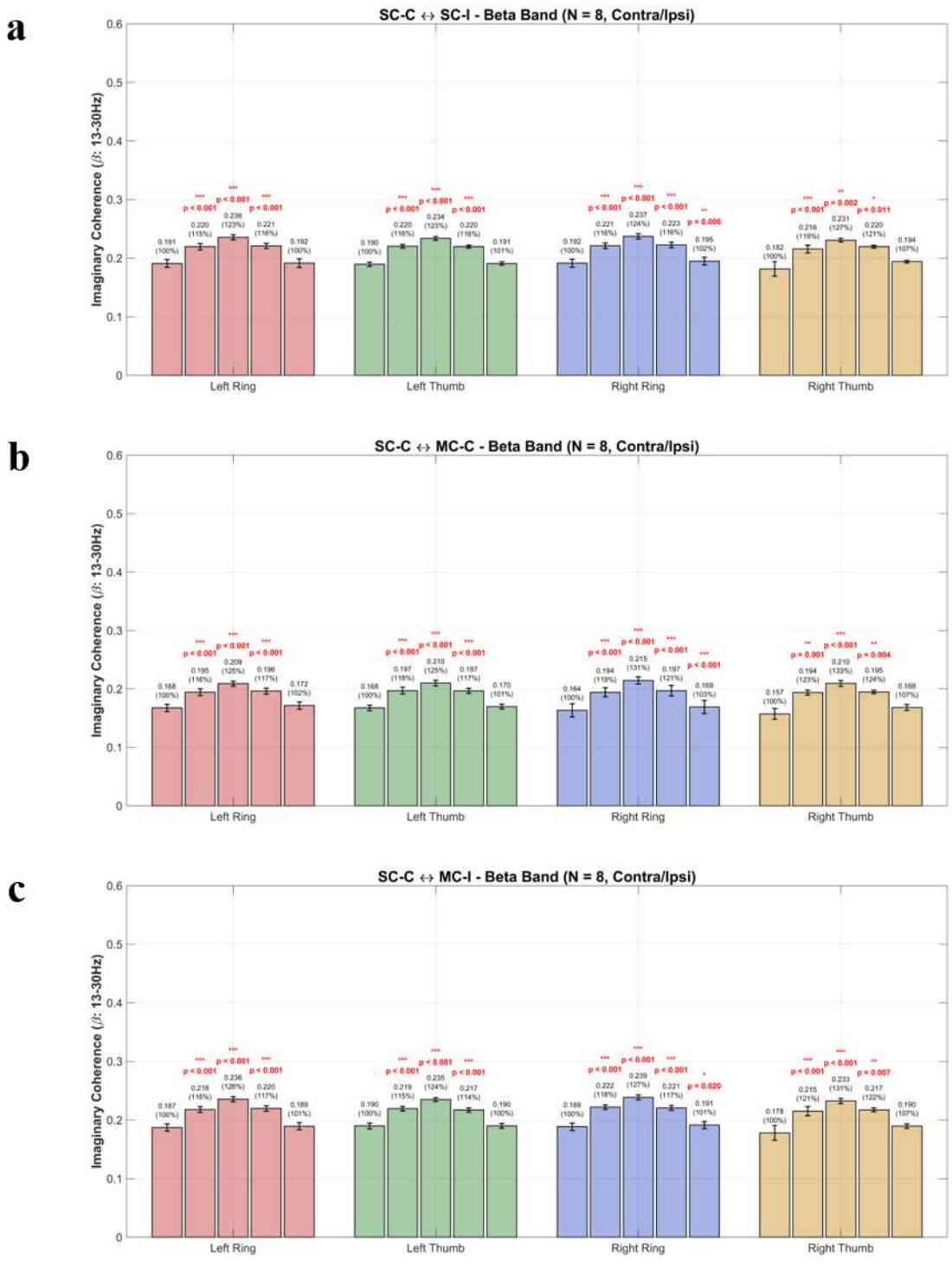

a
SC-C ↔ SC-I - Beta Band (N = 8, Contra/Ipsi)
b
SC-C ↔ MC-C - Beta Band (N = 8, Contra/Ipsi)
c
SC-C ↔ MC-I - Beta Band (N = 8, Contra/Ipsi)
Imaginary Coherence (β: 13-30Hz)
Left Ring
Left Thumb
Right Ring
Right Thumb

Figure 11